THESIS

L-TYPE CALCIUM CHANNEL-DEPENDENT SIGNALING IMPACTS GNRH RECEPTOR FUNCTION AND INTERCELLULAR COMMUNICATION IN CULTURED GONADOTROPES

Submitted by

Meggan L. Drennan

Department of Biomedical Sciences

In partial fulfillment of the requirements

For the Degree of Master of Science

Colorado State University

Fort Collins, Colorado

Summer 2020

Master's Committee:

Advisor: Gregory Amberg

Colin Clay
Deborah Garrity
Nicole Kelp

ABSTRACT

L-TYPE CALCIUM CHANNEL-DEPENDENT SIGNALING IMPACTS GNRH RECEPTOR FUNCTION AND INTERCELLULAR COMMUNICATION IN CULTURED GONADOTROPES

The hypothalamic-pituitary-gonadal (HPG) axis is a negative feedback biological system critical in fertility, reproduction and development. Gonadotropin-releasing hormone (GnRH) is first released by the hypothalamus and binds to GnRH receptors (GnRH-R) on gonadotrope cells of the anterior pituitary gland where the receptors must mediate a variety of pulsatile signals. The gonadotropin hormones, luteinizing hormone (LH) and follicle stimulating hormone (FSH), are subsequently released by the pituitary and act upon the ovaries and testes, further producing gonadal steroids to be circulated throughout the body. GnRH pulse frequency and amplitude determine successful gonadotropin release, which is ultimately regulated by the GnRH-R.

The GnRH-R is a heterotrimeric G-protein coupled 7-transmembrane domain receptor with Gα, β, and γ subunits. Ligand binding initiates an intracellular cascade that leads to a global increase of cytosolic calcium concentration by way of calcium influx through voltage-gated calcium (Ca_V) channels, and intracellular calcium release from endoplasmic reticulum (ER) stores. Gonadotropes depend on intracellular calcium concentration to carry out their specific physiological function, such as transcription of gonadotropin subunits, hormone biosynthesis and release.

Calcium flux is a normal and important aspect of cellular function, including cell-cell communication. Calcium oscillations have been well documented in multiple cell types, with different patterns being induced with distinct treatments. Observations in this line of research include the following: different oscillatory patterns lead to different physiological outcomes, the rate at which internal calcium is secreted from the ER can greatly impact these patterns, and IP3 receptor clustering on the ER results in localized changes in calcium concentration rather than a marked global difference, implicating a spatial stochasticity. These oscillations have shown evidence of paracellular coupling at gap junctions, as well as synchrony following extracellular diffusion.

Chapter two of this thesis details experiments investigating calcium oscillations using a membrane-targeted calcium indicator. Immortalized αT3-1 cells were transfected with a membrane-targeted GCaMP and TIRF microscopy was used to capture fluorescent calcium activity. Cells were treated with GnRH as well as various pharmaceutical treatments that would exploit L-type Ca_V channel function and manipulate normal intracellular calcium release. An array of observations was recorded. Qualitatively, there was an overall increase in calcium activity in the majority of cells after GnRH treatment. Drug-induced inhibition of calcium influx and intracellular calcium release diminished calcium activity entirely. Further, synchronized activity was captured among several cell groups, showing both pre-established synchrony and GnRH-induced synchronized peaking. Further research should be conducted to better understand the full mechanism underlying these behavioral responses, but these experiments provide a foundation for this work.

Chapter three highlights experiments using a GFP-tagged GnRH-R in αT3-1 gonadotropes in order to investigate GnRH binding-induced receptor mobility and clustering.

Treatment groups were identical to the previous chapter. SRRF and binary analysis were used to characterize receptor activity. Descriptively, clustering of receptors was seen, especially when calcium activity was limited, but more appropriate methods of quantitative analysis should be explored in order to go beyond these observations in processed images.

This thesis concludes overall that GnRH-induced calcium oscillation patterning and receptor clustering are far more complex and difficult to study than initially thought. Much more research is needed to determine any conclusive findings, however, these experiments may serve as a stepping stone toward obtaining the answers sought.

ACKNOWLEDGEMENTS

This process has been truly challenging and opened my eyes to a whole new approach to science. I feel very fortunate and grateful to have had the opportunity to study and grow under the guidance of Dr. Greg Amberg here at CSU. The insight, expertise, as well as humanity he brought forth as an advisor was unparalleled. I thank him for taking me in and allowing me to make mistakes and learn in the process. There were incredibly difficult moments, but his constant caring and understanding made a world of difference. There are a number of others without whom I never could have been successful, and to those individuals, I want to extend a heart-felt “thank you” for everything they have done.

Upon joining the lab, An Dang was the first to show me the ropes, generously giving up her precious time to teach me how to properly culture cells and care for materials and equipment. Jimmy Singh also lent his time and effort to ensure that I was making the right moves and fully understood the experimental procedures I was carrying out. Heather Szerlong was absolutely pivotal to my training in cell culture, molecular techniques, and overall understanding of cellular processes of particular lab interest and focus. Time and time again, she put aside her own priorities to help me learn and further my education. I genuinely do not know how I would have achieved success without her guidance. Experimental conception and preliminary data for chapter one is fully credited to Heather. I cannot thank her enough for her mentorship.

To my friend and peer, Huda Alqahtani, thank you for the never-ending moral support, for talking with me through data interpretation, and for the nonstop encouragement. I am so lucky to have met you and had the opportunity to work next to you for two years.

Thanks to my committee for being flexible, supportive and willing to take me on as a student. Thank you to the BMS department and graduate school for working around family and personal circumstances during my time in the program. A special thank you to Brittany Runyan for her incredible work as our department administrator and always going above and beyond to ensure that we have all of the information and resources we need.

Finally, I want to express the most overwhelming gratitude for my husband and baby girl, who have kept me going every day, always shining light on the positive. Your support saved me at times. You make every minute of this worth it and I would be absolutely lost without you both.

TABLE OF CONTENTS

Chapter 1: Background

1.1 HPG Axis and Gonadotropin Hormones

The hypothalamic-pituitary-gonadal (HPG) axis is a negative feedback biological system critical in fertility, reproduction and development. As the name suggests, the system consists of communication between the hypothalamus in the brain, the pituitary gland and the gonads. The pituitary gland is home to several cell types which have distinct behaviors given their functional role in the system. Gonadotrope cells, located in the anterior pituitary, produce gonadotropin hormones which trigger a cascade of events essential for proper function of the HPG axis. These cells are stimulated by activation of receptors specific to gonadotropin releasing hormone (GnRH), secreted by the hypothalamus. The gonadotrope is vital to the performance of the HPG axis as the cell must coordinate several responses to GnRH stimulation and then carry out appropriate processes (Dang et al., 2014). Once the cells are stimulated, the gonadotropin hormones luteinizing hormone (LH) and follicle stimulating hormone (FSH) are released from the pituitary and will act upon the ovaries and testes, further producing gonadal steroids to be circulated throughout the body.

Gonadotropin hormones are both produced by pituitary gonadotrope cells and are dimeric, differing only in their β-subunits, FSHβ and LHβ. When paired with their α-subunit (αGSU), they become operational and crucial chemicals that determine healthy development, fertility and reproduction. Both hormones have specific roles in males and females, initiating further production of sex steroids and processes necessary for reproduction. In females, LH initiates androgen production in follicular Thecal cells. Later on, LH also controls granulosa cell production of progesterone. FSH prompts granulosa cells in the ovaries to begin production of estradiol by enzymatic conversion of Theca-produced androgens. In males, LH promotes

generation of testosterone and androgen-binding protein in testicular Leydig and Sertoli cells. FSH binds to Sertoli cells in order to trigger production, proliferation and maturation of sperm cells (Bliss, Navratil, Xie, & Roberson, 2010).

1.2 Gonadotropin Releasing Hormone (GnRH)

There are at least two isoforms of GnRH that exist in humans and have been extensively studied, cleverly named GnRH-I and GnRH-II. Although these two isoforms, and the 21 others that have been identified in different organisms, diverge in function and location, the decapeptide structure is highly conserved across species (Chowdhury & Sridaran, 2009). GnRH-I is primarily released by the hypothalamus to act on the anterior pituitary, but has been found in other reproductive tissues as well. In the pituitary, we know that GnRH-I regulates the production and secretion of gonadotropin hormones, but outside, it may play a role in autocrine and paracrine regulation in reproductive tissues as well as the immune system (Cheng & Leung, 2005). GnRH-II is different in that it is located in both central and peripheral tissues, and its activity was long thought to be mediated through the type I GnRH receptor, (as a type II receptor had not been identified in humans for a long period of time). Apart from the pituitary, GnRH-II has shown to support multiple actions in peripheral tissues, including inhibition of tumor growth (Cheng & Leung, 2005; Chowdhury & Sridaran, 2009). Studies have also shown that this isoform can cause robust gonadotropin release in primates, likely through the type I GnRH receptor (Densmore & Urbanski, 2003).

Since gonadotropes produce two distinct hormones, controlled expression of receptors as well as protein subunits is maintained through pulsatory GnRH secretion (Bliss, Navratil, Xie, & Roberson, 2010; Chowdhury & Sridaran, 2009; Tsutsumi & Webster, 2009). The hypothalamus is therefore continuously releasing GnRH in pulses between 30-120 minutes, depending on the

time within a cycle (Chowdhury & Sridaran, 2009). LH and FSH are produced and secreted in a pattern determined by this fluctuating stimulation in order to regulate proper gonadal development and function. GnRH pulse frequency and amplitude allow for successful gonadotropin release, and is shown to be cyclically alternated with LH given its negative feedback process (Tsutsumi & Webster, 2009). For this reason, it is critical that GnRH secretion is accurate and concise in frequency, duration and concentration.

Dysfunctional release can have severe consequences, as multiple studies have shown. For instance, when pulses drop too low, amenorrhea and infertility can be seen. While sustained, high-frequency pulses are linked to issues such as polycystic ovarian syndrome (PCOS; Bliss, Navratil, Xie, & Roberson, 2010; Hall, Taylor, Hayes, & Crowley, 1998; Reame et al., 1985). Further, in clinical observations, continuous stimulation by GnRH lowered natural production of gonadotropin hormones (Bliss, Navratil, Xie, & Roberson, 2010). This suggests that proper pulsatility of GnRH lends itself to proper sensitivity of gonadotropes and subsequent communication with gonads. Given the significance of the global physiological response elicited by GnRH, many therapeutic interventions for fertility specifically target gonadotropic cells (Dang et al., 2014; Tomao et al., 2014).

1.3 GnRH Receptor and Signaling

As gonadotropin activity is initiated by GnRH, focus on the GnRH receptor (GnRH-R) is important in order to better understand subcellular events that occur leading to normal and abnormal function or pathology within the system. Only one wildtype GnRH-R (type I) has been identified and confirmed in humans, although there are additional subtypes that exist in other vertebrates. The type I GnRH-R is a heterotrimeric G-protein coupled receptor (GPCR) with seven transmembrane domains and Gα, β, and γ subunits. While its extracellular terminal domain

and transmembrane domains are typical, the GnRH-R has an uncommon structural difference in its cytoplasmic terminal domain. Rather than the classic carboxyl terminal tail, the mammalian GnRH receptor has a short intracellular end with only 2 amino acids, altering its functionality. Compared to other GPCRs, the GnRH-R is internalized much slower, and therefore desensitizes much more slowly as a result of the short tail (Rispolli & Nett, 2005; Willars et al., 1999). Delayed desensitization could be beneficial if not necessary in receiving varying pulsatory GnRH signals controlling ovulation and development.

Upon ligand binding, $G\alpha_q$ subunits activate phospholipase-C (PLC) and Phosphatidylinositol 4,5-bisphosphate (PIP2) is cleaved, forming inositol trisphosphate (IP3) and diacylglycerol (DAG) (Naor, 2009). Each of these second messengers plays a role in increasing calcium activity within the cell. DAG stimulates protein kinase C (PKC) activity, triggering heightened calcium influx through voltage-gated calcium (Ca_v) channels (*see Figure 1.1 on the following page for visual representation**; Dang et al., 2018; Stjilkovic, Bjelobaba & Zemkova, 2017). IP3 binds to an internal receptor and initiates calcium release from the endoplasmic reticulum (ER) where intracellular calcium is stored in gonadotropic cells (Stojilkovic, Tabak & Bertram, 2010). Ultimately, all of the afore-mentioned events culminate in the calculated increase of calcium both intracellularly from the ER, and through membrane-bound Ca_v channels.

More globally speaking, these events are known to be crucial to the systemic activation of follicular maturation and ovulation in females. In order for ovulation to occur, there must be an increase in the production and biosynthesis of LH, known as the LH surge (Plant, 2015; Dang et al., 2018). This enhanced production necessitates the activation of L-type Ca_v channels and extracellular signal-regulated kinase (ERK), a mitogen-activated protein kinase (MAPK) that

reliably increases after GnRH stimulation of gonadotropes (Dang et al., 2018; Grosse et al., 2000; Mulvaney, Zhang, Fewtrell, & Roberson, 1999). Measurement of ERK activity

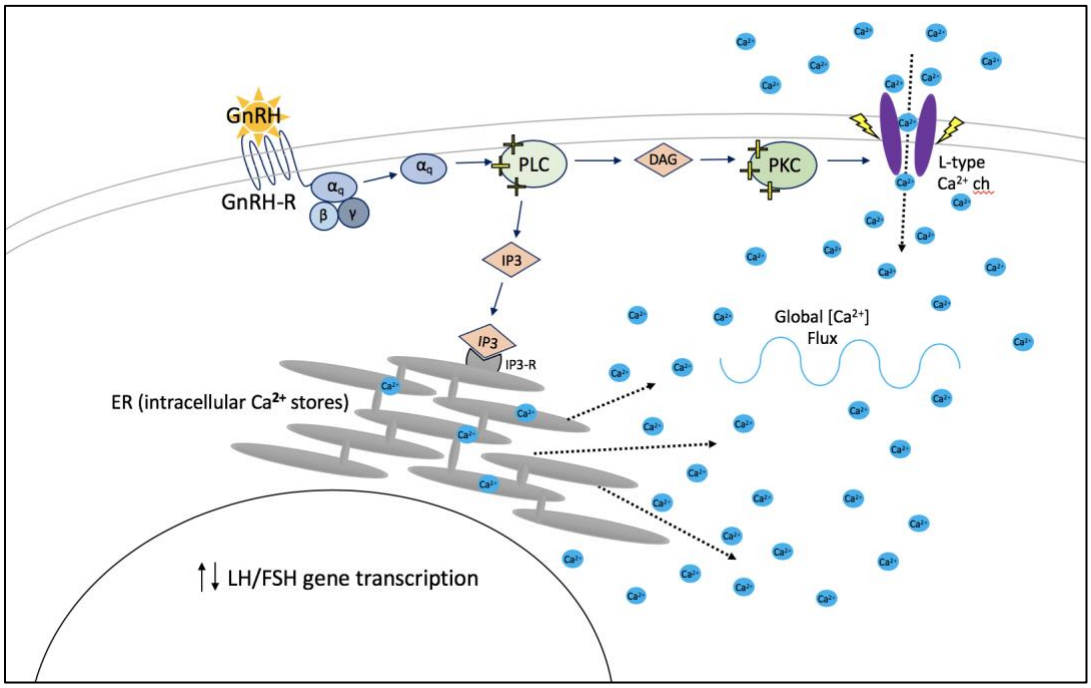

***Figure 1.1 Model of GnRH ligand signal cascade and calcium flux response.**

and that of other specific MAPKs are studied in gonadotropes as they transmit signals to the nucleus based on membrane voltage activity, thereby modifying gene transcription of essential proteins and gonadotropin hormones (Mulvaney & Roberson, 2000). Activation of these kinases is especially responsive to pulsatile GnRH, allowing for regulation of pulse frequency to the nucleus (Campos et al., 2018). Disruption of any of these steps can interrupt the event sequence and impede normal gonadal function. Furthermore, misfolding and other flaws in the expression of the GnRH-R can cause disorders such as hypogonadotropic hypogonadism, demonstrating the larger implications of understanding normal receptor function (Themmen & Huhtaniemi, 2000).

1.4 GnRH-induced Calcium Signaling

Gonadotropes are excitatory cells that depend on intracellular calcium concentration to carry out their specific physiological function. Electrical signaling events at the cell membrane

generate the influx of calcium through Ca_v channels, specifically L-type channels. Multiple types of voltage-gated calcium channels exist and are classified according to their structure and gating properties, as well as location. L-type Ca_v channels are characterized by slow inactivation, making their effects long-lasting. Calcium currents are determined by structurally different α1 subunits that can be divided into three groups: Ca_v1, Ca_v2 and Ca_v3 (Catterall, 2011). L-type calcium currents are moderated by the Ca_v1 subunit type. The α1 subunit contains four homologous domains, each of which is made up of six transmembrane sections, known as S1-S6. Each domain's S4 segment acts as the voltage sensor and undergoes a conformational change that opens the pore, allowing for calcium entry (Catterall, 2011). This channel opening is necessary to trigger action potentials as well as the release of intracellular calcium, both of which are important in producing transient calcium currents that regulate the transcription and release of gonadotropin hormones (Campos et al., 2018; Stjilkovic, Bjelobaba & Zemkova, 2017).

Calcium influx through specific Ca_v1 channels can cause calcium-induced calcium release (Catterall, 2011). Additionally, smaller calcium transients occur spontaneously, but are too small to accomplish hormone release (Stojilkovic et al. 2005). Instead, the frequency of these transient increases in concentration determine gene expression and transcription of gonadotropin subunits. Specifically, the LHβ subunit transcription is responsive to high frequencies, while low frequency increases trigger transcription of the FSHβ subunit (Campos et al., 2018; Melamed et al., 2012).

Further, unlike other neurons, exocytosis and thereby hormone release from pituitary gonadotropes is found to be predominantly initiated by a quick release of calcium from the ER (Campos et al., 2018). When IP3 binds its intracellular receptor on the ER, it acts as a calcium channel in its own right by causing a conformational change of the receptor and subsequently

releasing sequestered calcium into the cytosolic space (Aguilar-Rojas, Pérez-Solis, & Maya-Núñez, 2016). This cytosolic accumulation of calcium then affects the voltage at the membrane, activating L-type Ca_V channels, but at sub-threshold levels, preventing action potentials from taking place. It is the sharp and sudden global increase of intracellular calcium that stimulates vesicular fusion and gonadotropin hormone secretion in these cells (Aguilar-Rojas, Pérez-Solis, & Maya-Núñez, 2016; Campos et al., 2018). Transient calcium activity is consequently pivotal to the functional dynamics of the cell.

Calcium is also a known regulator of structural architecture in different cell types. It governs neuronal migration by influencing cytoskeletal remodeling, and plays a role in cell motility, adhesion, cytokinesis and stabilization (Dalghi, Ferreira-Gomes, & Rossi, 2018). In immune cells, calcium influx may help to organize actin filaments at the synapse by promoting depolymerization and spatially directing polymerization (Hartzell, Jankowska, Burkhardt, & Lewis, 2016). Conversely, cytoskeletal factors such as actin are shown to assist in functional regulation of intracellular calcium concentration via the plasma membrane calcium ATP-ase (Dalghi, Ferreira-Gomes, & Rossi, 2018). With calcium flux, actin dynamics lend themselves to interesting changes in cellular morphology, especially in TIRF microscopy where membrane adhesion and movement is so conspicuous.

The intricate calcium signaling process is specific so that even minor disruption can cause impaired global function. Environmental substances known as endocrine disruptors mimic the body's natural hormones and interfere with endocrine function. For example, when introduced in vitro, the commonly known chemical BPA increased cytoplasmic calcium concentrations proportional to the effects of estradiol (Ruffinatti et al., 2019). Increases like these can cause severe systemic disturbance that can lead to developmental issues such as cardiac

disorder (Lombo et al., 2015) and mammary cancer (Paulose, Speroni, Sonnenschein, & Soto, 2015). The importance of calcium signaling cannot be understated.

1.5 Oscillatory Calcium Flux

Since the 1980's, calcium oscillations have been well-documented, observed through patch-clamp electrophysiology and various calcium reporters (Beta & Kruse, 2017; Merelli et al., 1992; Powell et al., 2020; Thurley et al., 2012). In fact, it is widely accepted that these oscillatory signals can occur by way of receptor binding or spontaneous spiking, and that they convey specific messages downstream of initiation (Beta & Kruse, 2017). Calcium oscillations are generally measured as a sequence of spiking events caused by increased global calcium concentration (Powell et al., 2020). Oscillations are largely a product of the regulatory feedback observed upon stimulation of intracellular IP3 receptors creating calcium flux throughout the cell (Powell et al., 2020). This feedback, combined with the sequestering of cytosolic calcium results in observable "spikes and waves" in intracellular calcium (Beta & Kruse, 2017; Thurley et al. 2012). Notably, spontaneously firing gonadotropes generally exhibit low internal levels of calcium (Stjilkovic, Bjelobaba & Zemkova, 2017). Experimentally, oscillations can be observed with both cytosolic and membrane-specific fluorescent calcium markers, and different oscillatory patterns can be induced with distinct treatments in varying cell types.

In this body of research, some noteworthy observations have been made. First, different oscillatory patterns lead to different physiological outcomes (Fletcher, Sherman, & Stojilkovic, 2018). Pituitary action potentials will vary in amplitude, duration and frequency depending on the intra- and extracellular environment of the cell. Calcium influx via Ca_v channels influences intracellular calcium flux and relies much on the duration of the action potentials that occur. The shorter spikes that gonadotropes tend to exhibit do not have a lasting enough effect to alter

calcium levels within the whole cell, and thus result in an oscillatory pattern different than other pituitary cells (Fletcher, Sherman, & Stojilkovic, 2018). Second, the rate at which internal calcium is secreted from the SR/ER can greatly impact these patterns, whether it is a slow release or a quick dump (Tang & Zuo, 2017).

Finally, IP3 receptor clustering on the ER results in localized changes in calcium concentration rather than a marked global difference, implicating a spatial stochasticity which can be difficult to measure statistically (Powell et al., 2020). These clustering events respond to calcium concentrations in discrete locations rather than the global concentration within the whole of the cell. Because IP3 receptors are so important in the scheme of gonadotropic calcium signaling and the subsequent release of gonadotropin hormones, it is important to understand the spatial activity of the receptors and their response to cellular calcium flux.

Beyond observations of basic oscillations, synchrony in both spontaneous and chemically induced calcium fluctuation have been recorded in several cell types, including cardiac myocytes (Gu, Pan, & Xu, 2014), hepatocytes (Hofer, 1999), pancreatic islets (Zhang et al., 2008), and hippocampal, cerebellar, and cortical neurons (Dravid & Murray, 2004; Wang & Gruenstein, 1997), but to date, have not been observed in pituitary gonadotropes. In capturing these attuned oscillations, some cells have exhibited paracellular coupling at gap junctions, increasing sensitivity to localized intracellular increases in calcium (Hofer, 1999), while others achieved synchrony following extracellular diffusion.

Chapter 2: Intercellular Communication May Be Influenced by GnRH-induced Calcium Signaling Via Intra- and Extracellular Sources

2.1 Introduction

Given what we know about calcium oscillations in different cell types, and how calcium flux affects gene transcription, this process can be seen in gonadotropes and their production of various hormones. However, to date, there is no data to our knowledge that supports multi-cellular synchronous calcium waves in these cells. Calcium is ubiquitous as a second messenger, but must be manipulated to visualize and study. Experimentally, there are numerous ways to detect calcium activity in live cells, such as dyes or genetic modification.

GCaMP is a genetically encoded calcium indicator developed to easily study living cells and organisms by enabling the visualization of calcium via fluorescence. It is comprised of green fluorescence protein (GFP), calmodulin (CaM), and a small sequence from myosin light chain kinase (MLCK) (Nakai, Ohkura & Imoto, 2001). CaM is a protein that, in the presence of calcium, can bind up to four calcium ions. Its structure allows for a conformational change upon binding which will then bind the MLCK sequence, promoting absorbance of the excitation wavelength and activating GFP fluorescence. In the absence of calcium, this wavelength absorption is conformationally hindered and therefore only a dim luminance can be seen, if any (Nakai, Ohkura & Imoto, 2001; Wang, Shui, Kotlikoff & Sondermann, 2008).

While observing real-time calcium activity via total internal reflection fluorescence (TIRF) microscope in cells transfected with a GCaMP6f calcium indicator, some interesting behaviors were noted after introducing GnRH to the cells. These observations were able to be reproduced and thus, provided the foundation of the current study. Based on preliminary

recordings, we hypothesized that GnRH treatment will increase frequency and amplitude of transient calcium oscillations, eventually leading to coupling through synchrony in oscillatory patterns in cell groups. These patterns should be interrupted upon treatment of various pharmaceutical treatments affecting calcium influx and intracellular store release.

In order to fully explore these assumptions, accompanying questions must be answered. In living cells, there is constant transient calcium flux from both voltage-dependent channel influx and intracellular release, but it is unclear as to whether one of these avenues plays a more critical role in the oscillatory synchrony observed. This can be tested by inhibition and exploitation of regular calcium pathways. A plethora of pharmaceuticals exist to make this possible. Intracellularly, calcium can be prevented from release by the ER with IP3 receptor antagonists. Achieving a similar result, calcium ATPase inhibitors cause the ER to empty its calcium stores and then prevent the sequestering and continued storage of calcium for the duration of the drug's effect. At the plasma membrane, calcium channel activity can be manipulated by both agonists and antagonists. An L-type calcium channel agonist will override any normal voltage-induced effects and open the channels, allowing a free-flow of calcium ions into the cell. Conversely, a channel antagonist will prevent any calcium influx through these channels, keeping the intracellular calcium concentration low and flux to a minimum.

It is also unclear as to whether there is a limit to the number of gonadotropic cells that are able to become coupled/grouped. A study of LHRH neuron calcium oscillations recorded intermittent synchronous peaks of more than 57 neuronal and intermediary cells in vitro at a given time (Richter, Keen & Karasawa, 2002). It could be the case that large gonadotropic cellular networks such as this exist. It is equally possible that only a small number of cells communicate locally via oscillatory calcium signaling. The lab data preceding this paper

recorded no more than two cells oscillating in a synchronous manner over a length of time. Larger groups of cells must be observed in order to see the level at which these synchronous oscillations can occur.

2.2 Materials and Methods

Cell Culture

The Amberg lab was kindly gifted clonal αT3-1 gonadotropic mouse cells by Dr. Pamela Mellon from the University of California, San Diego. Researchers maintained these cells in HyClone high-glucose DMEM with 10% fetal bovine serum (Atlas Biologicals) and 1% sodium pyruvate (Invitrogen), incubated at 37°C in 5% CO_2 humidified air. All cells were used between passages 9-18. Researchers plated cells in standard 35mm glass bottom dishes that were coated and pre-incubated with a 1:250 dilution of Matrigel matrix (Corning) in high-glucose DMEM, and allowed to grow to approximately 30-40% confluency before transfection. The Qiagen SuperFect Transfection Reagent and protocol achieved cellular transformation with both plasmids of interest, after which cells were allowed to grow for 24-48 hours. Best results for all experiments occurred closer to 48 hours of cell growth with plasmid expression. Confluency of plates ranged from 50-85%. For all experiments, cells were serum-starved for 60-90 minutes.

To detect calcium activity at the cell's surface, cells were transfected with a plasma membrane-targeted slow-reacting GFP-tagged calcium sensor. This pGP-CMV-GCaMP6s-CAAX plasmid was purchased from Addgene, who received this gift from Tobias Meyer (Tsai et al., 2014).

Experimental Treatment

Researchers used FPL 64176 (FPL) as an L-type voltage-gated calcium channel agonist at a working concentration of 1μM. Nicardipine (Nic) acted in contrast, as an L-type voltage-gated

calcium channel antagonist, at a working concentration of 10nM. Thapsigargin (Thaps) acted as an inhibitor of endoplasmic reticulum Ca^{2+}-ATPase at a working concentration of 1μM. Upon treatment, the cell releases its internal calcium stores and further sequestering and storage is inhibited. The final working concentration of GnRH treatment was 10nM for all cells. All pharmaceuticals listed were purchased from Sigma-Aldrich and dissolved in dimethyl sulfoxide (DMSO), which was used as a control for treatment.

Microscopy

Images were captured with an Olympus IX83 total internal reflection fluorescence (TIRF)/epifluorescence microscope. All images were acquired with a 100x oil immersion objective and a 488nm excitation laser, using a Hamamatsu CMOS camera on the TIRF setting in Olympus cellSens software. Live cells were imaged primarily in Ca^{2+}PSS buffer, while some experiments used a calcium-free Mg^{2+}PSS buffer. All data shown can be assumed to have been imaged in Ca^{2+}PSS buffer unless specifically stated otherwise.

Researchers took a consecutive series of baseline images for each of multiple cells or cell groups over the course of several minutes, mapping and saving the location of each cell group. GnRH, DMSO or a drug of interest was then delivered to the dish at a final working concentration previously specified, and imaging resumed to gather post-treatment data. To allow for GnRH to take full effect, 5 minutes passed before beginning post-treatment imaging. After treatment, images were again taken of each cell group over the following 15 minutes before the cells were eventually either discarded, or treated with a second round of GnRH, pharmaceutical drug, or DMSO control. Exposure time for each GCaMP image sequence ranged from 150-300ms with no additional time between frames, and each image sequence contained between 800-2000 frames.

Analysis

Using ImageJ software, the researcher quantified fluorescence over time by selecting three regions of interest (ROI) and averaging the output for each frame. Data was then normalized and plotted with GGplot in RStudio. In order to remove excess noise, a moving average was taken and plotted over the original data. To quantify these data, measurement of peak frequency and amplitude was attempted using Clampex (pCLAMP) software, however these analyses proved inconclusive due to the variability and nature of the cells' activity. Rather, cell behavior is discussed in terms of clear observations within the plotted fluorescence data.

2.3 Results

To first test the GnRH treatment hypothesis, multiple cell groups within several dishes were imaged under the same conditions (n = 43). Cell group responses varied, even within the same culture dish. Table 2.1 breaks down the responses observed by percentage of cell groups analyzed. When compared to baseline calcium flux, GnRH caused the greatest percentage change by increasing both amplitude (or brightness of fluorescence) and frequency of calcium oscillation patterns. The next most noted change was an increase in amplitude of oscillations, but not frequency when compared to baseline activity. In contrast, the third most observed response

Table 2.1 Descriptive breakdown of cell group responses to GnRH treatment when compared with baseline recordings. (n = 28) Fluorescence plots were assessed for patterns of amplitude and frequency, and revealed a widespread array of calcium activity upon stimulation.

Calcium Oscillation Behavior	% of cells
Increased amplitude & frequency	28%
Increased amplitude only	23%
Increased frequency only	9%
Decreased amplitude & frequency	2%
Decreased frequency	9%
Decreased amplitude	19%
No notable change	9%

to GnRH was, oddly, a decrease in oscillation amplitude alone, with no other notable effects. Careful study of the following representative plots reveals the differential responses to various treatments in cell pairs and groups imaged over time, including existing and GnRH-induced synchrony of calcium activity in two or more cells.

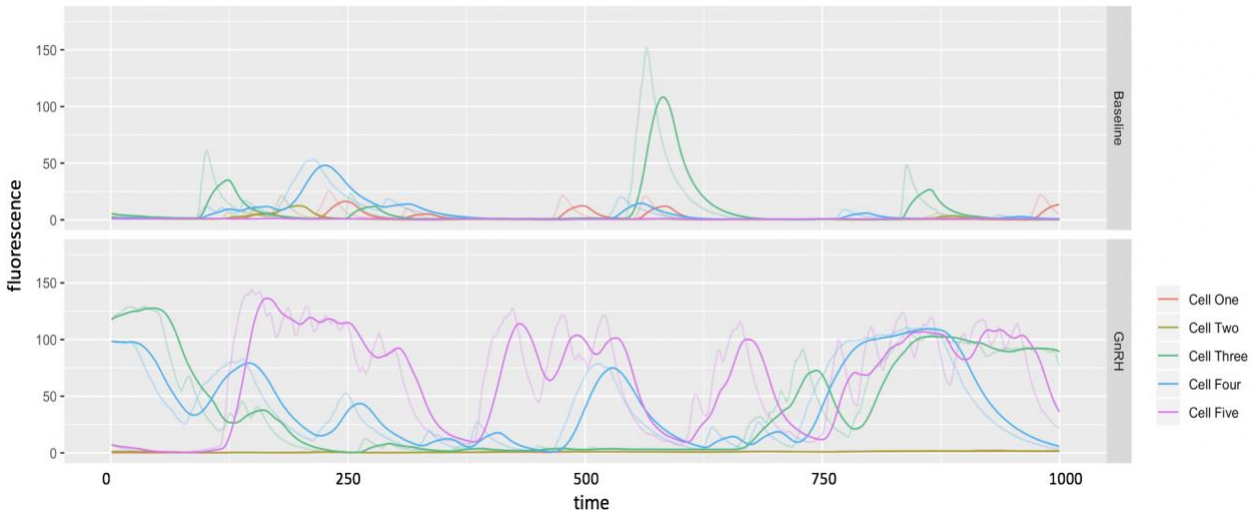

Figure 2.1 Increased amplitude and frequency of calcium oscillation peaks with GnRH stimulation. 1000 frames of five cells taken over the course of 2:30. Baseline activity can be seen four of the five cells imaged. Post-GnRH, cells three, four and five increase in peak activity, while cells one and two are undetectable.

As increased amplitude and frequency of oscillation peaks was the most commonly observed response to GnRH, these plots were assessed for the number of active cells and other notable behaviors. Figure 2.1 demonstrates this effect initially in two of five recorded cells, and a third eventually showing increased activity as well. The remaining two cells are silent after GnRH treatment. It is also worth noting that generally overall effects and trends are discussed, but there are other subtle observations that can be made within cell groups. For instance, cell one (orange) does show some activity, although minimal, in the baseline recording, but falls completely silent post-GnRH. Additionally, cell three (green) shows a large spike among other smaller spikes in the baseline recording, so its activity in the post-GnRH plot may or may not be

induced by the hormone treatment. Finally, the cell with no detectable activity in the baseline plot shows the most robust response to GnRH in both amplitude and frequency.

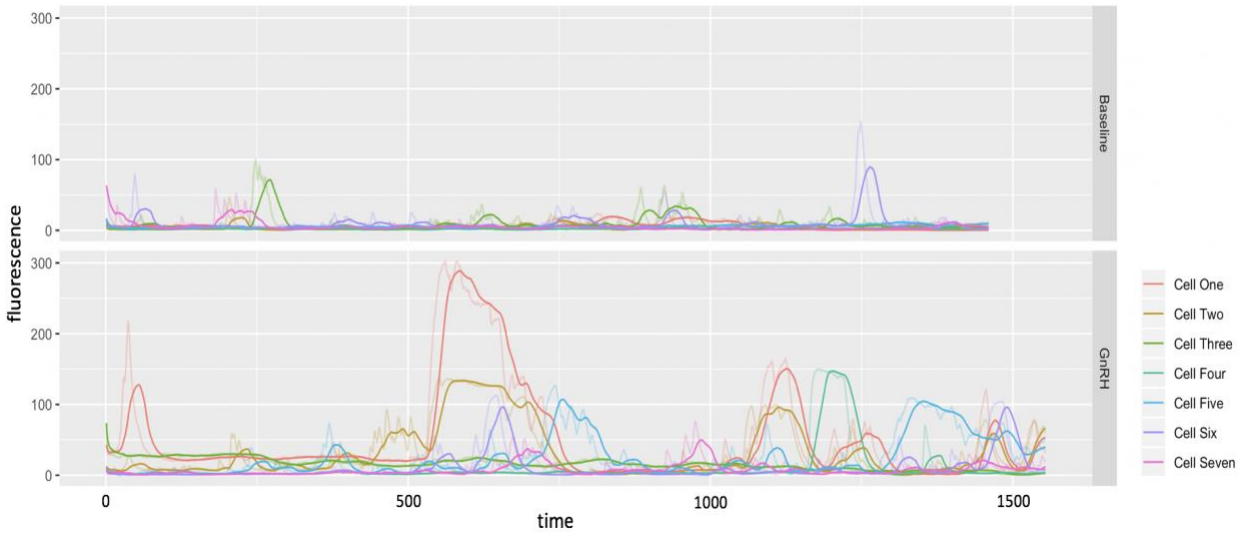

Figure 2.2 GnRH-induced increase in amplitude. 1500 frames of seven cells taken over 3:45. All cells are actively displaying calcium flux during baseline recording. Peak amplitude increases in six of the seven cells captured. Cells one and two demonstrate some synchronized peaks 12 minutes after GnRH treatment.

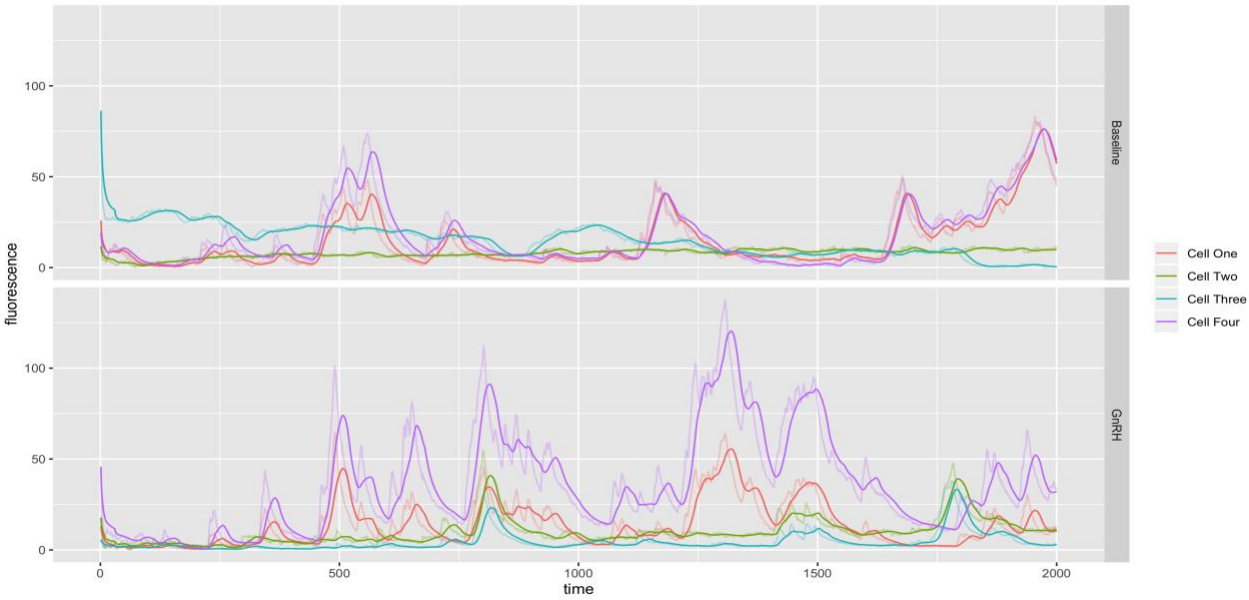

Figure 2.3 GnRH-induced increase in amplitude and frequency, established synchrony. 2000 frames taken over 4:00. GnRH causes and increase in intracellular calcium activity in cells 1 & 4. Cells 2 & 3 are recruited into the established synchronous oscillation pattern.

Increased amplitude alone was another commonly recorded response to GnRH treatment from baseline. A representative sample is shown in Figure 2.2, with several cells showing strengthened responses in calcium flux to the hormone. Only one cell (cell four) showed the opposite effect, with decreased peaking. With this number of cells in a given group, it was expected that at least two would begin to exhibit synchronous activity. Indeed, after GnRH treatment, cells one and two show a number of synchronized peaks throughout the recording. While there are a few other cells' peaks that coincide with the two synchronized cells, the characterization of those peaks does not suggest recruitment into that pattern. There were a great deal of cell groups that fell into this category – some cell's calcium activity would increase in amplitude with or without synchrony, while other cells within the same image would dim or cease oscillating altogether. With these mixed reactions, all were noted, and the most abundant effect helped to categorize the group.

Alongside increased overall calcium activity, recruitment of cells into previously paired group oscillatory patterns occurred frequently. The level of activity varied substantially from group to group, but one, two, and even three cells at a time were recruited from minimal activity to fully synchronized peaking. Figure 2.3 highlights one of these particular episodes, in which two previously paired cells begin to recruit two additional cells into their synchronized oscillations. Although the peaks are not perfectly synchronized in this image sequence, the effect is easily seen, as any previous cell activity in the baseline recording lacked any predictable pattern. These cells (two and three) also peak together once more, independently of cells one and four, which may suggest GnRH-induced pairing.

While established synchrony in paired cells was seen in many dishes, occasionally multiple cells would present perfectly synchronized oscillations that were amplified with GnRH.

Often, these grouped cells demonstrated low-level calcium activity that was maintained over the duration of observation. With GnRH treatment, all cells within the grouping produced an increase in calcium flux, continuing to oscillate in sync with each other. Representative data for this observation can be seen in Figure 2.4.

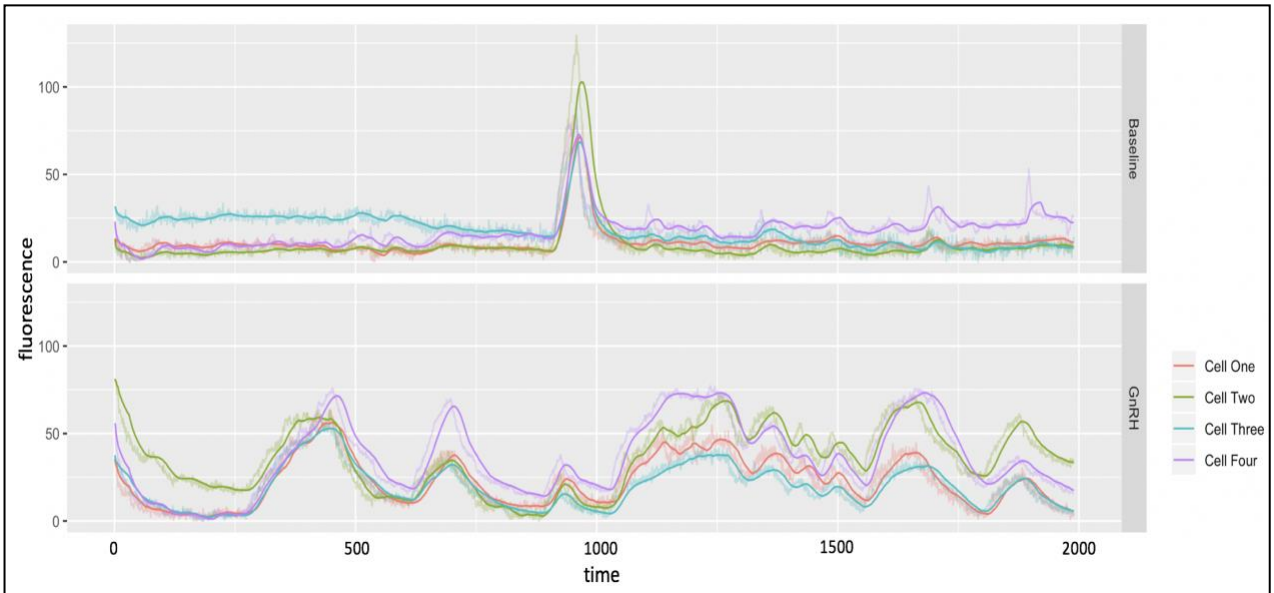

Figure 2.4 GnRH-induced increase of calcium activity in cell group with established synchrony. 2000 frames of four-cell group taken over 3:20. All cells oscillate in synchrony at a low-level amplitude prior to any hormone treatment. After GnRH treatment, cells remain synchronous but amplitude and frequency of oscillation peaks increases.

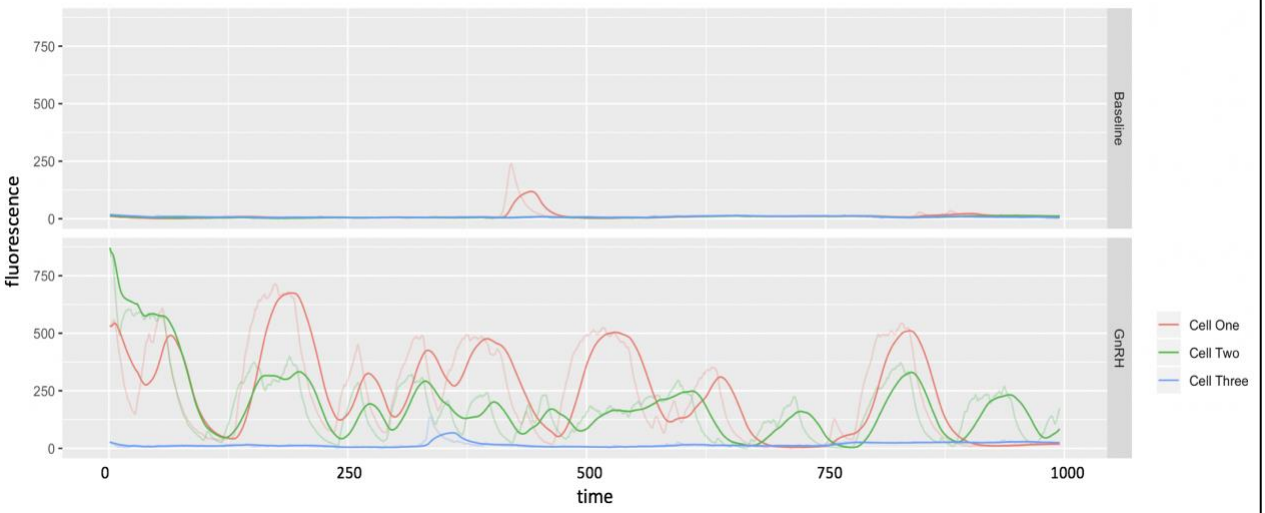

Figure 2.5 GnRH-induced synchrony with increased calcium activity 1000 frames taken over 2:30. Cells one and two demonstrate GnRH-induced increase in calcium activity, and synchrony 12 minutes post-treatment.

After completion of data collection, cell groups were analyzed not just for synchrony, but the type of synchrony that was taking place. As previously noted, certain cell groups were already established and exhibiting synchronized oscillations, while synchrony was obviously induced by GnRH in other groups. Nearly 40% of all cell groups showed some level of synchronous calcium activity in response to GnRH. Of the cells that showed these synchronous patterns, 59% of these were established groupings (23% of total cells observed), or groups that were synchronous prior to GnRH, while 41% were hormone-induced (16% of total cells observed). As predicted, the most frequent occurrence of GnRH-induced synchrony was observed between just two cells rather than multiple. Figure 2.5 highlights two cells coordinating oscillations after GnRH stimulation. While these patterns are not perfectly synchronous like those seen in established pairs, there is clear synchrony in most oscillatory peaks.

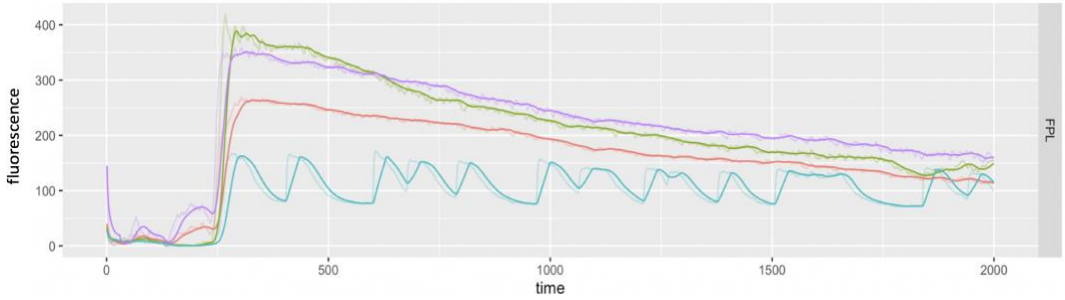

Figure 2.6 FPL Treatment. 2000 frames over 5 minutes. Fluorescence spikes as L-type Ca_V channels are forced open, causing a sudden and large influx of calcium. (See Figure 2.3 for baseline and GnRH treatment of same cell group.)

After becoming familiar with the various effects GnRH has on calcium flux in transfected αT3-1 cells, we explored various pharmaceutical manipulations affecting cytosolic calcium flux. FPL treatment opened L-type Ca_V channels, causing an obvious spike in intracellular calcium concentration (see Figures 2.6, 2.7) and providing further validation of successful plasmid expression (n = 21). Recovery of GnRH-induced oscillatory calcium signaling after FPL was attempted, but unsuccessful. Fluorescence faded over time, likely as an effect of photobleaching,

but calcium flux did not return to normal within the experimental time frame. However, in a small number of cell groups, some cells continued to show consistent fluctuation, as seen in Figure 2.6, differing from baseline and post-GnRH recordings. Other plots show a sort of "flickering" as fluorescence spikes with calcium influx (see Figure 2.7), but again, this is not akin to typical calcium flux.

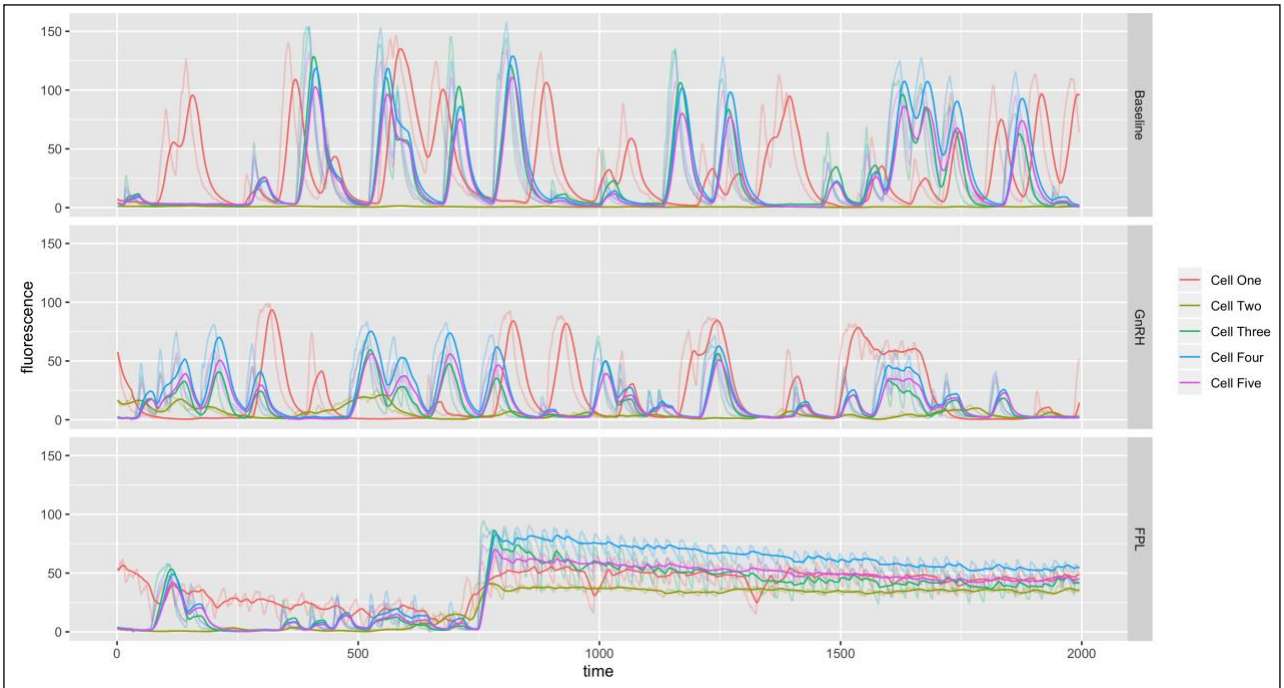

Figure 2.7 FPL Treatment. 2000 frames over 5:00. Forced activation and opening of L-type Ca_V channels causes calcium influx from extracellular environment, causing fluorescence) to spike and sustain as the GFP-bound indicators become saturated.

To observe the counter effect, Nic was then used to instead block all L-type Ca_V channels, preventing calcium influx. Upon treatment, spontaneous calcium spiking ceases almost immediately (see Figure 2.8). In this condition, recovery of calcium flux was also attempted after Nic treatment, but was unsuccessful for the duration of experimental observation. The effect was the same regardless of whether the cell had undergone GnRH treatment previous to Nic exposure. Once the cells were treated with Nic, fluorescence diminished, although some cells demonstrated longer reaction times to the drug.

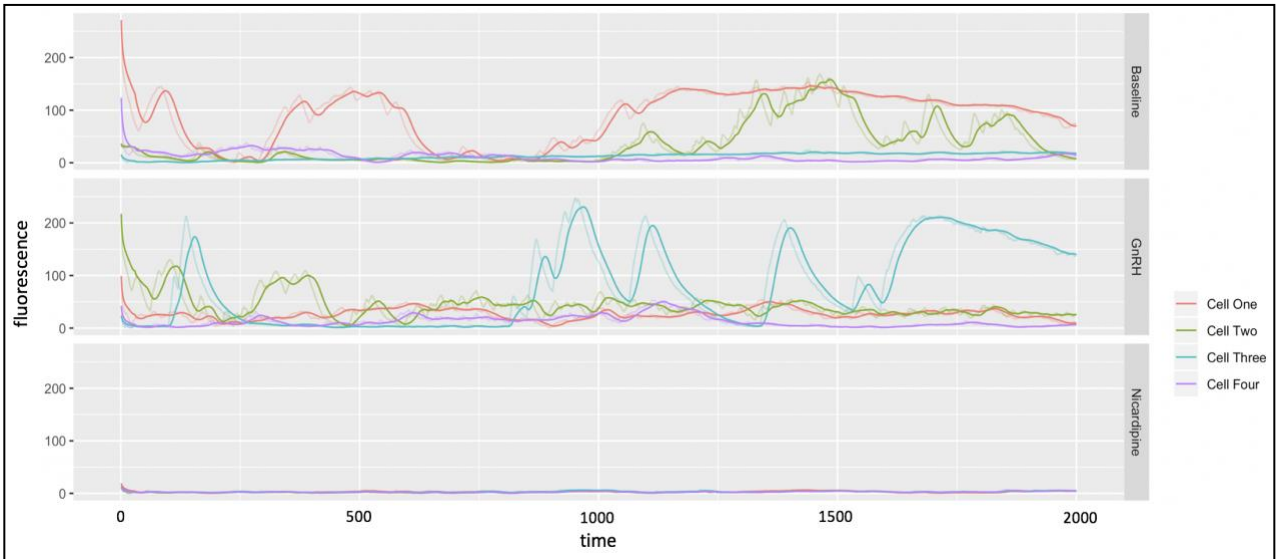

Figure 2.8 Nicardipine Treatment. 2000 frames over 5:00. Global hindrance of L-type Ca_V channels prevents calcium influx from extracellular environment, dimming fluorescence to virtually zero.

This all changes, however, when cells are pre-incubated with Nic. A small group of dishes were left to incubate in serum-free media with 10nM Nic for 15 minutes before imaging. The same concentration of Nic remained in the imaging media as well in order to keep consistent pressure on cells throughout the experiment. Observations under these conditions were unexpected. In baseline recordings, where the cells have been consistently exposed to Nic, rather than a flatline indicating a lack of calcium flux, perfectly synchronized oscillations were seen in every dish. Unlike regular baseline recordings, GnRH did not appear to have a marked or consistent effect on these cells' calcium activity, but the cells remained synced and demonstrated a constant intracellular flux (see Figure 2.9).

Based on this behavior, we used Thaps to manipulate the normal release and storage of intracellular calcium by the ER. This drug was applied to cells a number of different ways. First, it was added to the dish after acquiring baseline data, followed by GnRH as the final treatment of those cells. A second method involved acquiring baseline and post-GnRH data, and then ending

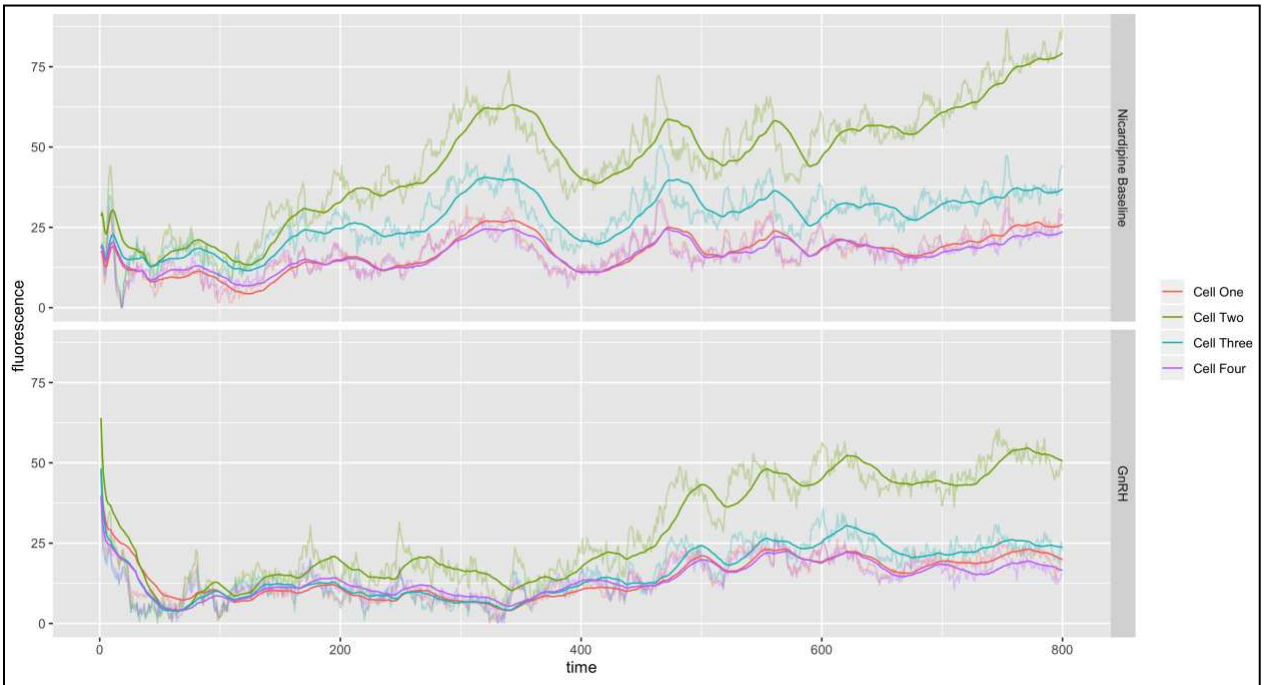

Figure 2.9 Nicardipine pre-incubation. 800 frames over 3:20. Baseline plot represents cells that were pre-incubated with Nicardipine for 15 minutes and then imaged in Ca_{2+}PSS buffer with 10nM Nicardipine. Cells were treated with GnRH and recorded 10 minutes later.

the experiment with Thaps treatment. Finally, following the method used for Nic above, cells were pre-incubated with 1μM Thaps in serum-free media for 15 minutes. After the incubation period, media was replaced with imaging buffer containing the same concentration of Thaps.

In the first treatment group, when cells were treated with Thaps after GnRH, calcium activity was almost entirely muted after a large spike reflecting the full release of calcium stores from the ER (n = 6). Like Nic, there were occasional delays in full elimination of fluorescence, but ultimately all cells diminished to near zero (see Figure 4.10). As with the other treatment conditions, recovery of oscillatory calcium activity was attempted by adding GnRH to the dish after Thaps treatment. Figure 4.11 illustrates this sequence of events. Baseline recordings were typical, with some active fluctuation in fluorescence. Labeled arrows show approximately when treatments were delivered to the dish, Thaps at ~frame 400. The calcium dump from the ER can

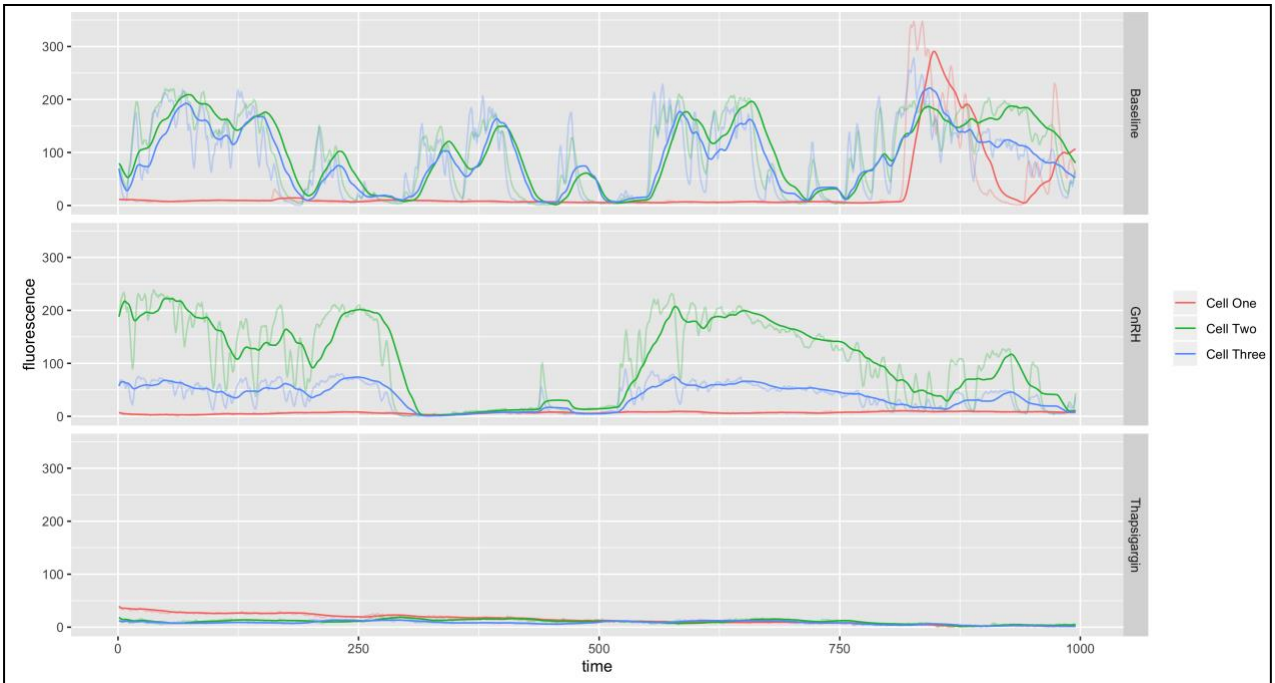

Figure 2.10 Thapsigargin Treatment. 1000 frames over 4:10. Cells two and three present established synchrony that is maintained after GnRH treatment, yet altered (i.e. dampened peak frequency). Upon treatment of Thapsigargin, calcium activity is abated.

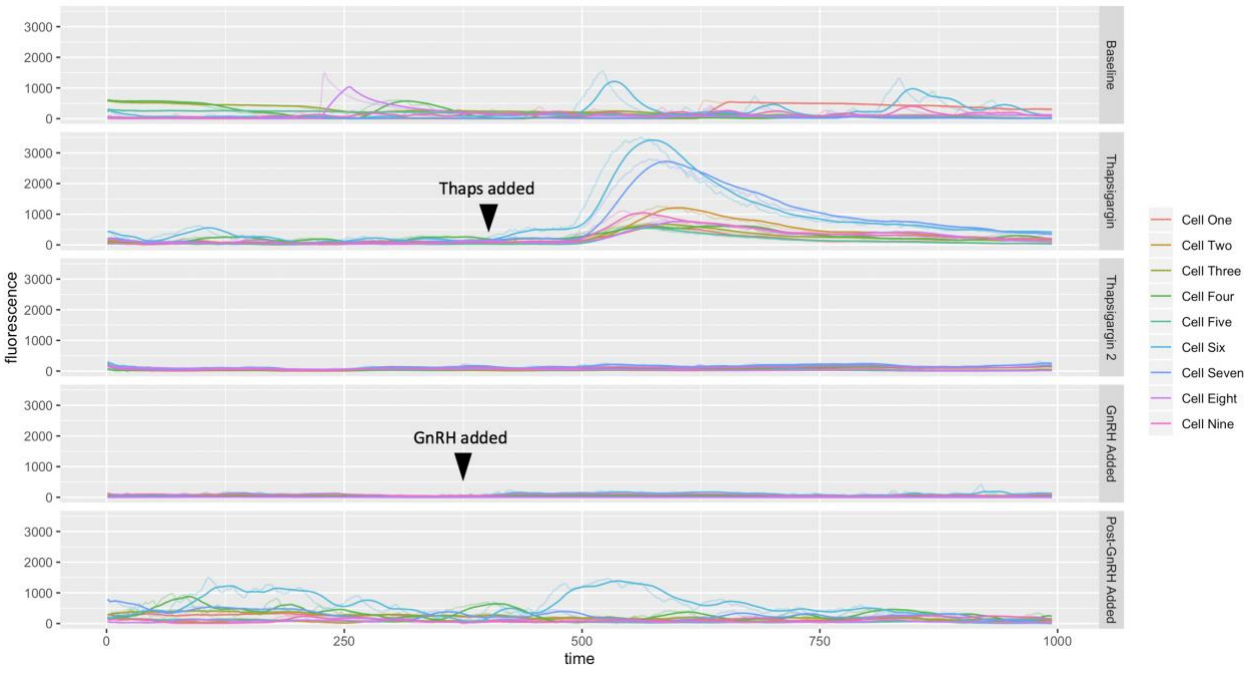

Figure 2.11 Thapsigargin Treatment with GnRH-induced recovery of calcium activity. 1000 frames over 4:00. Baseline image sequence in Ca^{2+}PSS buffer with no treatment. Second image sequence shows live cell response to Thapsigargin treatment during imaging, revealing the sudden and total release of calcium from the ER. Third recording shows lack of calcium flux after Thaps treatment. GnRH was added during a fourth round of imaging. After 5 minutes, a final recording revealed recovered activity in a number of cells, reflecting baseline levels.

be seen just after drug treatment, followed by a full 4 minute sequence of minimal activity. The labeled arrow indicates that GnRH was delivered around 10 minutes post-Thaps treatment (~frame 370), and soon after, low-level fluctuations can be seen. Within minutes, GnRH-induced recovery is successful and calcium activity is back to baseline amplitude levels, although fluctuation pattern and spiking activity is different from baseline.

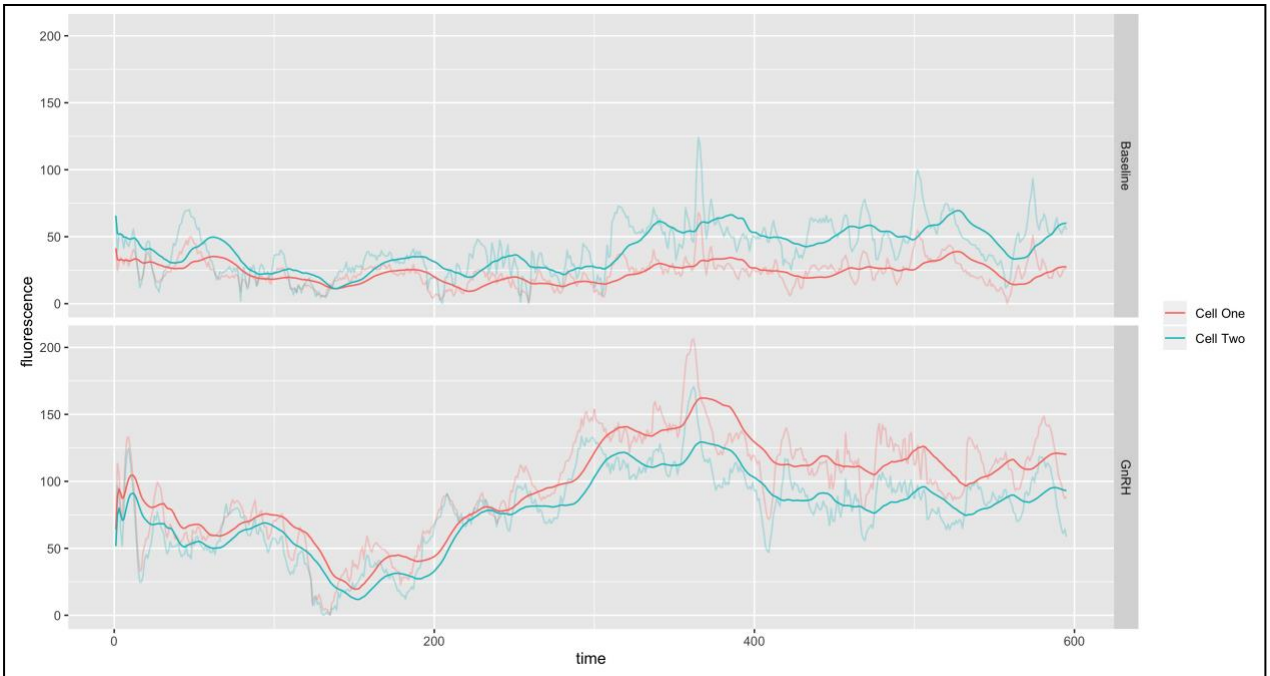

Figure 2.12 Thapsigargin pre-incubation, Mg^{2+}PSS. 600 frames over 3:00. Baseline recording represents cells pre-incubated with Thapsigargin for 15 minutes and imaged in calcium-free Mg^{2+}PSS buffer with 1μM Thapsigargin. After baseline reading, cells were treated with GnRH and recorded 10 minutes later.

Finally, pre-incubation was tested and imaged in both calcium-free Mg^{2+}PSS buffer, as well as Ca^{2+}PSS buffer. Sequences of cells imaged in calcium-free buffer revealed similar data to the Nic sequences, showing perfectly synchronized calcium fluctuation, prior to and after treatment of GnRH (see Figure 2.12). This was true for each dish imaged in this condition (n = 4). Cells imaged in calcium differed vastly in their response, with no specific spiking pattern, but an increase in amplitude of fluorescence in some cells when GnRH was introduced (see Figure 2.13; n = 4).

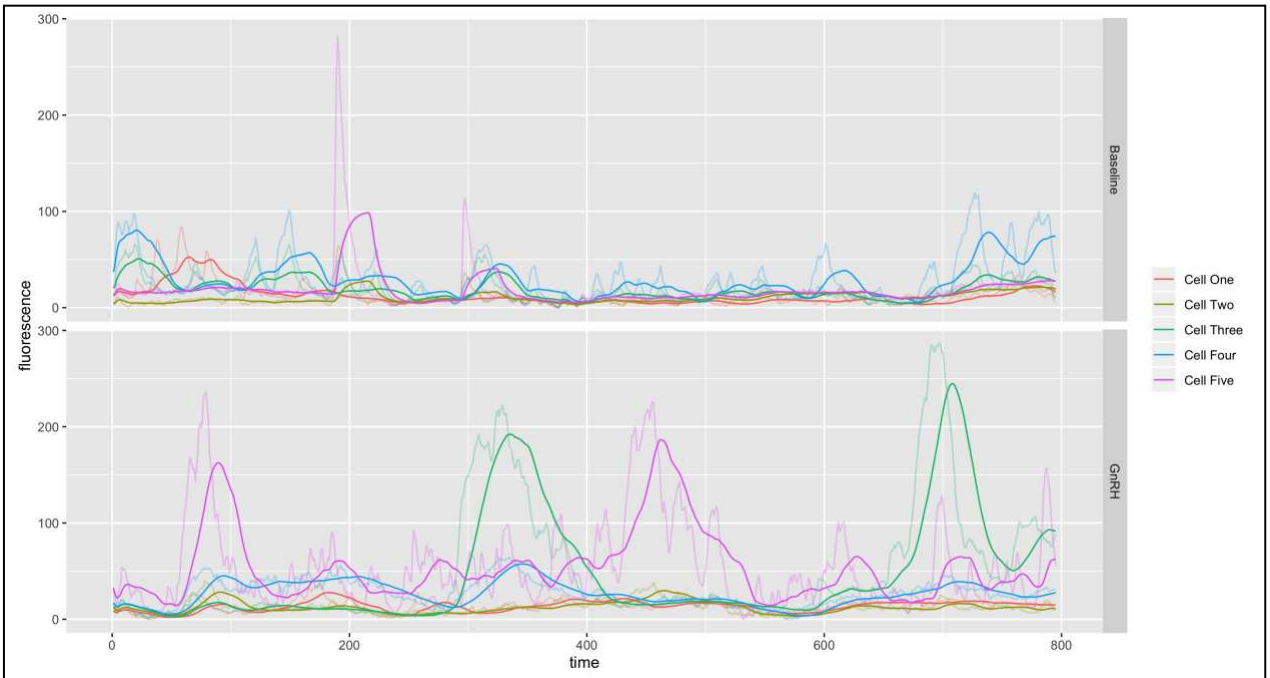

Figure 2.13 Thapsigargin pre-incubation, Ca^{2+}PSS. 800 frames over 4:00. Baseline recording represents 15-minute pre-incubation with Thapsigargin and imaging in Ca^{2+}PSS buffer with 1μM Thapsigargin. After baseline, cells were treated with GnRH and recorded 10 minutes later.

2.4 Discussion

Overall, it can be said that GnRH increases calcium activity a majority of the time, whether it is both amplitude and frequency, or amplitude alone. This increase in intracellular calcium concentration was expected given what we know about gonadotropes and GnRH stimulation. The patterns of synchrony however were not as expected and displayed a much larger scale of variability than anticipated based on preliminary findings. Part of this can be explained by lack of control conditions in the present study. Previous experiments investigating calcium activity were conducted in single isolated cells under the extreme control of voltage-clamp. Original assumptions regarding calcium activity were largely derived from these highly controlled studies. Given that the current research sought to observe calcium activity of cells in a more natural environment, the only controls researchers had were cell growth, the aqueous environment of the cells and the course of treatment used.

Before this experiment, it was unclear how much of a role was played by the release of intracellular calcium stores. After attempted recovery experiments, it may be concluded that while intracellular calcium release from the ER does contribute to these oscillations to a degree, consistency and amplitude is much more dependent on calcium influx through L-type Ca_v channels. Inhibition of the SERCA pump caused a delay in response to GnRH, but did not prevent oscillations from returning to normal once cytosolic calcium was built back up again. In contrast, recovery of normal calcium activity was not possible when L-type Ca_v channels were blocked. Although there did remain slight activity in some cell groups, the vast majority saw almost no activity after Nic treatment. In short, intracellular calcium release may add to oscillatory signaling, but L-type Ca_v channels mediate the amplitude of the oscillatory pattern to a much greater degree.

In several cases, images showed varying sites of increased calcium concentration (i.e. brighter fluorescence) within cells after treatment rather than uniform global increase. This observation could be explained by localized intracellular calcium release leading to influx through calcium channels in discrete locations at the membrane. In cells treated with Thaps, these brighter areas were located around the perimeter, which makes sense as the calcium is entering the cell at the membrane. Another observation seen especially in cells treated with Thaps was an obvious calcium flow, or movement of wave-like fluorescence into and through the cell. Descriptively, it looked like the calcium was being pulled inward from the membrane toward and more central location. This again makes sense when considering the fact that without intracellular calcium release, a cell may compensate by increasing influx through Ca_v channels in order to maintain proper function. (See supplementary material)

In these experiments, the maximum number of cells recorded in established synchronous patterns was six. In these established groups, calcium activity increased a majority of the time after treatment of GnRH, possibly reinforcing the existing communication. However, in pairs of cells that displayed coupled activity, disruption of synchronous peaking was observed a number of times after GnRH treatment. This could be due to a number of factors, the most obvious of which is that even the most successful transfection will not affect 100% of cells. An experiment looking at cell communication in local groups may capture a network in which some cells are unaffected by laser excitation. In this case, we would not see the full spectrum of activity upon hormone treatment.

Additionally, multiple recordings showed a switch in communicating cells within groups after GnRH application. For example, in a baseline recording of four cells, perhaps cells one and four show synchronous peaking, but after GnRH exposure, calcium activity shifts and then cell four becomes inactive while cells one and three display synchronous peaking. This is another possibility that may not have been fully captured in every cell group given the lack of perfect GFP expression. Finally, confluency of cells seemed to make a difference in some oscillatory signaling and synchronous behavior. This could not be clearly parsed out in the current study due to incomplete documentation of plate confluency. It was noted, however, that synchronous patterns did tend to increase with higher cell density, which may provide some insight into establishment of network communication/synchrony. All recordings of pre-established synchrony were taken from dishes with confluency greater than 60%.

The largest groups that exhibited GnRH-induced synchrony consisted of four cells, several of which were recruited by cells already engaged in synchronous activity. Expansion of cellular communication networks could be a possible effect of GnRH activation. However, aside

from groups with established synchrony, the highest level of synchronous activity was seen most reliably in cells which were somehow deprived of normal calcium influx. Specifically, cells treated with Nic, pre-incubated with Nic, and pre-incubated with Thaps and imaged in calcium-free buffer showed near perfect synchronicity in calcium flux. Both FPL and Nic affect intracellular calcium concentration, and therefore impact IP3 binding and ER release that leads to cytosolic flux. However, with these displays of perfect synchronicity coming from cells that are unable to bring in calcium through L-type Ca_V channels, it is confounding that cell-cell communication is somehow increased. This puzzling observation should be more thoroughly investigated in future experiments. Our current understanding is that the underlying mechanism is complex and likely involves both voltage-dependent and voltage-independent fluctuations in intracellular calcium, as well as influx through L-type channels and release from intracellular stores. Perhaps low-level calcium activity, or even localized low calcium concentration causes cells to synchronize in order to attempt to maintain proper function.

Ultimately, cellular communication via calcium activity is likely much more complex than what we predicted, and further research is necessary to fully explore and understand the underlying mechanisms and intricacies of paracellular network communication. A number of follow-up experiments have been proposed and should be conducted in order to expand our understanding of these initial observations. First and very simply, Thaps and Nic should be used simultaneously to reproduce conditions seen in dishes pre-incubated with Thaps and imaged in calcium-free buffer. Other pharmaceutical manipulations can be used to observe cellular responses, such as EGTA, a calcium chelator, EDTA, a magnesium chelator, as well as an effective calmodulin inhibitor, such as Calmidazolium.

To expand on observations from this set of experiments, it could be interesting and potentially advantageous to analytically look at directionality of calcium flow and whether it is insightful to communication between cells. Since the calcium indicator used in the present experiments is membrane-targeted, a GCaMP construct that targets cytosolic calcium could be a useful comparison for activity. Furthermore, a calcium indicator that is fast-reacting may draw attention to observations that the current construct is not able to illuminate. Finally, in the setup of our lab's new microscope, a perfusion system has been created that would allow for the seamless replacement of buffers during live imaging. The system would make it possible to introduce pre-diffused treatments to cells and then remove and replace with wash buffers, etc. It would also allow us to create baseline recordings of cells in a regular calcium buffer, but remove and replace it with calcium-free buffer in order to observe speed and characteristics of cell behavior and response.

Chapter 3: Receptor Mobility and Cellular Movement: Differential and Complex Responses to Hormone Stimulation in Pituitary Gonadotropes

3.1 Introduction

The cell's plasma membrane was thought for a period of time to be completely fluid, allowing for free movement of its subparts. While this model is not entirely wrong, it is now widely accepted that membrane composition and distribution of proteins and receptors may be managed by lipid microdomains, or rafts. These are small, dynamic spaces within the membrane, dense with sphingolipids and cholesterol, which serve the purpose of organization and specific functionality of cell types (Navratil, Bliss & Roberson, 2010; Sezgin, Levental, Mayor, & Eggeling, 2017; Simons & Vaz, 2004). With the rafts, fluidity of the membrane remains but is limited by the spatial properties of the microdomains. This model also allows for the study of heterogeneity within membrane structure, and potentially furthers the understanding of receptor movement and behavior at the cell membrane. Lipid rafts in αT3-1 gonadotropes have been identified and are thought to play an important role in downstream receptor signaling, impacting healthy ovulation and fertility (Navratil et al., 2003; Navratil, Bliss & Roberson, 2010).

Researchers suggest that GnRH-Rs exist independently until they are ligand-bound, at which point they begin to assemble into larger groups (Horvat et al., 2001). Solitarily, the receptors move rapidly across the membrane surface until GnRH or other agonists are present. Upon ligand binding, receptors being to aggregate, forming larger clusters that demonstrate much slower mobility. This is suggested evidence of organizational grouping into lipid rafts, where mobility becomes far more limited (Horvat et al., 2001). Within this model, it would be expected that under experimental conditions with GnRH, receptors would create distinct

groupings on the plasma membrane within these rafts, and that these groupings would remain more spatially stable given their limited mobility.

Structurally speaking, it makes sense that lipid rafts, along with their embedded proteins, would require support from within the cell, especially if conditions call for cellular movement. Cytoskeletal support has been studied in the context of GnRH-induced gonadotropic movement, and points to the significance of actin and cortactin in mobility and hormone release (Navratil et al., 2007; Navratil et al., 2014). Studies consistently show an array of subtle to extreme morphological changes upon GnRH stimulation, much that can likely be attributed to actin dynamics. When normal actin function was manipulated, both cell mobility and normal intracellular signaling with GnRH were impaired (Navratil et al., 2007). With striking morphological changes being observed in the presence of GnRH, there are likely interesting changes to be noted upon treatment of the drugs being used in the present experiments as well.

In an attempt to characterize GnRH-R behavior after hormone activation, we used a GFP-tagged GnRH-R to take images of cells before and after GnRH and other pharmaceutical treatments. We hypothesized that in the presence of GnRH, receptors would mobilize and cluster together in measurable groups on the plasma membrane of αT3-1 cells. Fluorescence should be less dispersed on the cell's surface after treatment when compared to baseline, and show a larger overall surface area when membrane area is accounted for. Additionally, there will likely be notable morphological changes, possibly differing between experimental groups.

3.2 Materials and Methods

Identical materials and methods as those mentioned in the previous chapter were used for this set of experiments. The same pharmacological treatments and concentrations, cell maintenance protocol, and microscope parameters were used to obtain the following data.

Cell Culture

A GFP-tagged GnRH receptor plasmid was developed and gifted to the Amberg lab by Dr. Colin Clay, and used to image over-expressed GnRH receptors in gonadotropes. The efficacy of this plasmid was previously validated by the lab of origin (Horvat et al., 2001).

Analysis

The Olympus cellSens imaging software was used to subtract background and two-dimensionally deconvolute images. These processed images were then imported to ImageJ where Super-resolution Radial Fluctuation (SRRF) analysis, a method used to distinguish true events from artifact and background, was performed with the FIJI plugin. SRRF output images were processed once more to obtain binary data by setting an event threshold of 60% and converting the image to mask. Once obtained, binary image data was measured for total area and number of receptor sites, or clusters (see Figure 3.1). All measurements are presented in arbitrary units (au).

Area output (in pixels) was normalized by dividing by 5000. To account for variability in surface area of cell membrane appearing in TIRF images, cell footprints were traced in ImageJ and the area measured. Finally, binary images were run through a K means cluster analysis using RStudio in order to track the distribution of fluorescent receptor sites. This technique was only partially successful and will be discussed further later on in this chapter.

Experimental Treatment

Pharmaceutical drug concentrations and dilutions for these experiments are identical to the previous chapter and served the same purposes. Pre-incubation of Nic and Thaps was followed by imaging in buffer containing the same concentration of the respective drug so as to maintain chemical pressure on the cell throughout the experimental procedure.

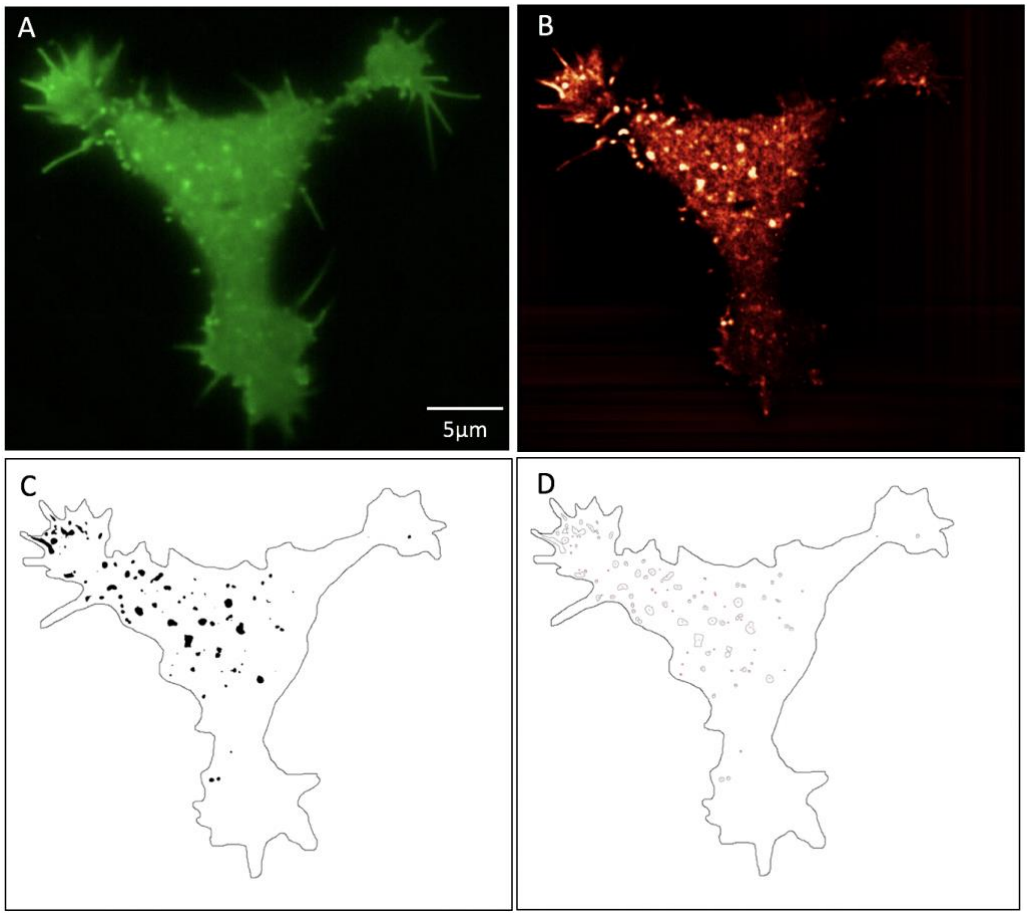

Figure 3.1 Representative images demonstrating method of analyses. A, Mean image of 100-frame sequence stack with background subtraction. B, Image output after completed SRRF analysis. C, Binary image at threshold of 60% with cell footprint overlay. D, Particle outline of receptor cluster spots analyzed for pixel area.

Microscopy

Researchers took a consecutive series of baseline images for each of multiple cells or cell groups over the course of a few minutes, mapping and saving the location of each cell group. GnRH was then delivered to the dish at a final working concentration of 10nM, and 5 minutes passed before imaging resumed. Another set of images were taken of each cell or cell group over the following 15-30 minutes before they were eventually discarded. The most notable changes occurred between 12-18 minutes post-GnRH treatment, so this was the targeted time frame for optimal imaging. For GFP-receptor image sequences, exposure time ranged from 150-300ms

with no additional time between frames, and each image sequence contained between 100-300 frames.

3.3 Results

Upon breakdown of the receptor imaging data, we determined the most relevant data points to look at were the total area of the cell, the area of receptor clusters, and the number of receptor clusters in a given cell area. These data are listed in Table 3.1 according to treatment group and the overall direction of change. As with the previous experiments, cells were treated with GnRH (n = 28), Nic (n = 13), FPL (n = 13), Thaps (n = 6), Nic pre-incubation (n = 4), and Thaps pre-incubation (n = 12). Data showed a decent split in cell responses to each condition, with the most robust being an increase in total cell area, decrease in receptor cluster area, and decrease in receptor clusters/cell area. Interestingly though, the cells that displayed the opposite effect – increases in receptor cluster area and receptor clusters/cell area – tended to have more extreme changes than the decreases.

Table 3.1 Summary of cell and receptor response to hormone and pharmacological treatment. Data represents the number of cells whose response to the given treatment either increased or decreased in area of membrane in TIRF images, normalized binary cluster area, and normalized binary receptor cluster data over membrane area in TIRF images. Nic and FPL responses are in reference to previous GnRH data point.

Treatment	Total Cell Area		Receptor Cluster Area			Receptor Clusters/Cell Area	
	Increase	Decrease	Increase	Decrease	No Change	Increase	Decrease
GnRH	21 (75%)	7	8	19 (68%)	1	11	17 (61%)
Nic	8 (62%)	5	5	8 (62%)	0	4	9 (69%)
FPL	3 (23%)	10	4	9 (69%)	0	6	7 (54%)
Nic BL + GnRH	4 (100%)	0	0	4 (100%)	0	1	3 (75%)
Thaps BL + GnRH	8 (44%)	10	7	11 (61%)	0	6	12 (67%)

A total of 28 cells are included with baseline (BL) and post-GnRH images, their responses to hormone treatment, in the form of number of receptor clusters over cell area and

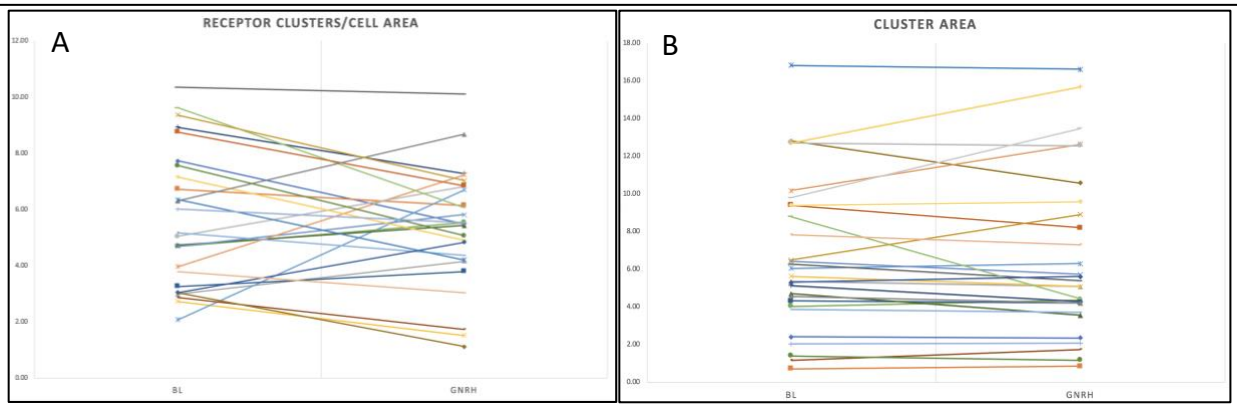

Figure 3.2 Representative data of receptor response to GnRH from baseline control image in calcium buffer. A, Normalized data showing number of receptor clusters over total membrane area in TIRF image from baseline (BL) sequences and after GnRH treatment. B, Normalized binary data showing total receptor cluster area before and after GnRH treatment. Colored lines represent individual cells.

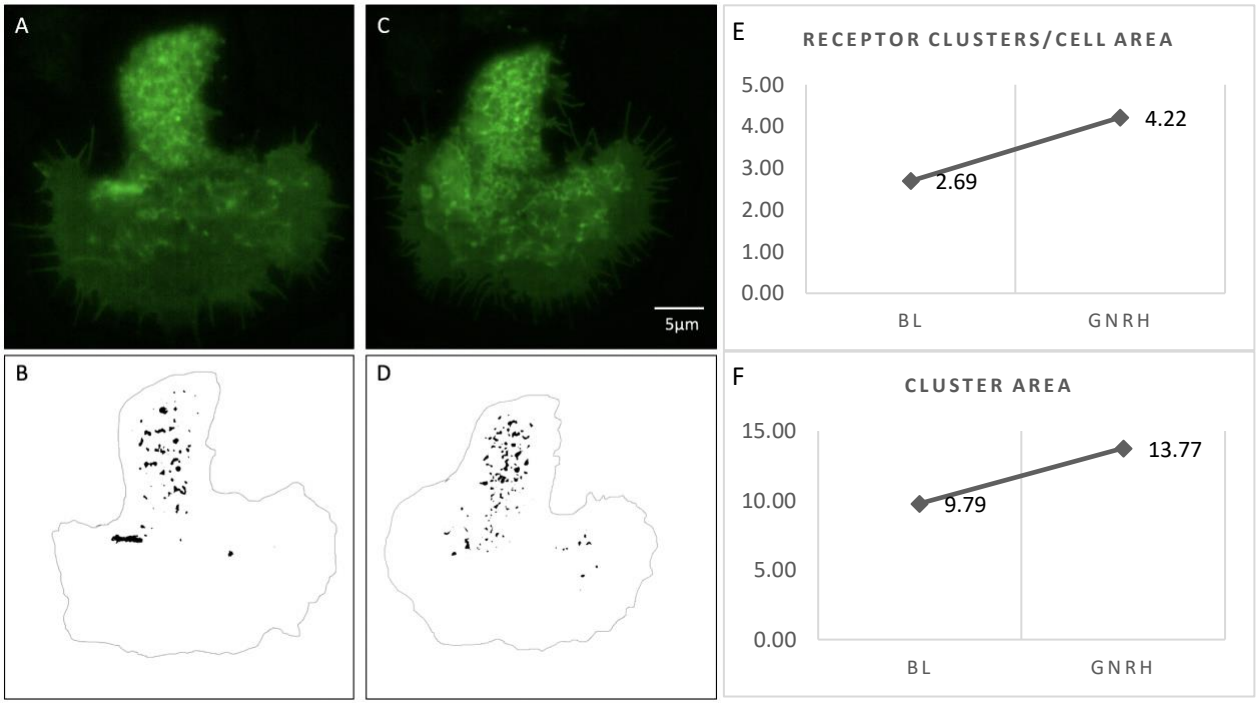

Figure 3.3 Representative images of cell response to GnRH treatment A-B, Respective fluorescent and binary images of baseline receptor activity on cells imaged in calcium buffer. C-D, Identical cell 12 minutes post-GnRH treatment. E, Visual representation of the cell's number of receptor clusters over total TIRF membrane area for baseline activity in calcium buffer, and 12 minutes post-GnRH treatment. F, Cell's total cluster area for baseline activity and post-GnRH treatment.

total receptor area, are illustrated in Figure 3.2. Figure 3.3 highlights a cell which underwent this treatment and showed an increase in both of these measures. While this cell had the more uncommon response to treatment, it is a good representation of receptor redistribution after the hormone is introduced. This was a typical occurrence, regardless of direction of change. Receptors were clearly mobile and showed clear patterns of redistribution after treatment on nearly all cells that were imaged, whether it was a cell area that had little or no receptors prior to treatment or otherwise. This example also demonstrates a small level of morphological change from BL to post-GnRH.

Interesting observations surfaced when drug treatment began. The first pharmaceutical to be used was Nicardipine. Calcium is fundamental in cell signaling and the downstream cascade of GnRH-R activation, so there was sure to be a noticeable effect when L-type Ca_v channels were blocked. Figure 3.3 illustrates the overall response of cells to both GnRH and Nic treatment in number of receptor clusters over cell area and total cluster area. Again, these data were altogether inconclusive. However, as expected, there was a visible change in receptor distribution and assembly after treatment (see Figure 3.4). While total receptor area in this image decreased with Nic (E/F) when compared to baseline (A/B), the sizes of existing clusters are notably larger than the previous images and indeed, less dispersed. The number of clusters per area also decreased from baseline, but the receptor clusters are larger. Although it is not as obvious in the GnRH-treatment condition (C/D), it can also be said that receptor clusters are visibly increasing in size, even slightly.

A second example (figure 3.6) is included to again demonstrate the consistency of this reaction to GnRH and Nic treatment. After GnRH (C/D), receptors begin to surface in a

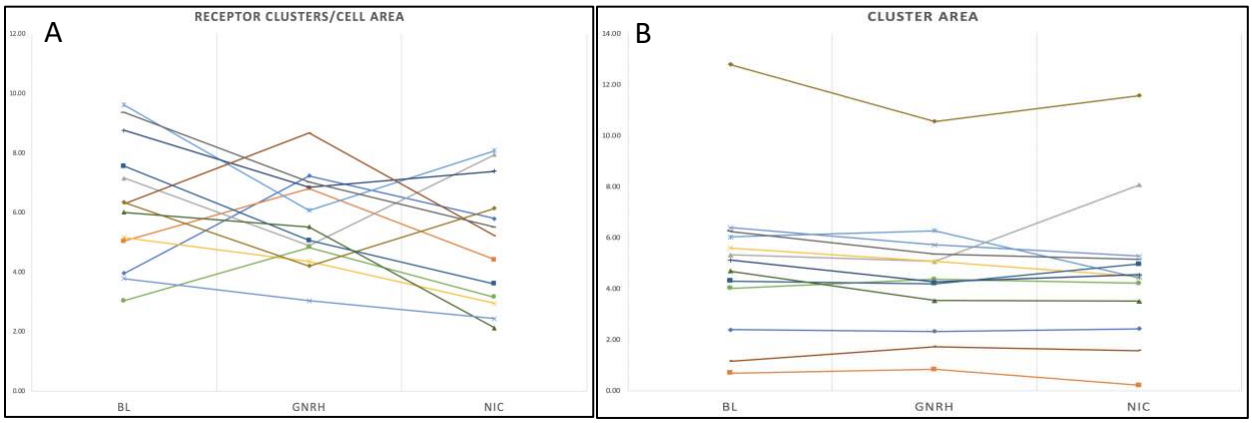

Figure 3.4 Representative data for receptor response to GnRH and Nicardipine from baseline control images in calcium buffer. A, Normalized data showing number of receptor clusters over total membrane area in TIRF image from baseline (BL) sequences, post-GnRH treatment, and post-Nic treatment. B, Normalized binary data showing total receptor cluster area for baseline, post-GnRH, and post-Nic treatment. Colored lines represent individual cells.

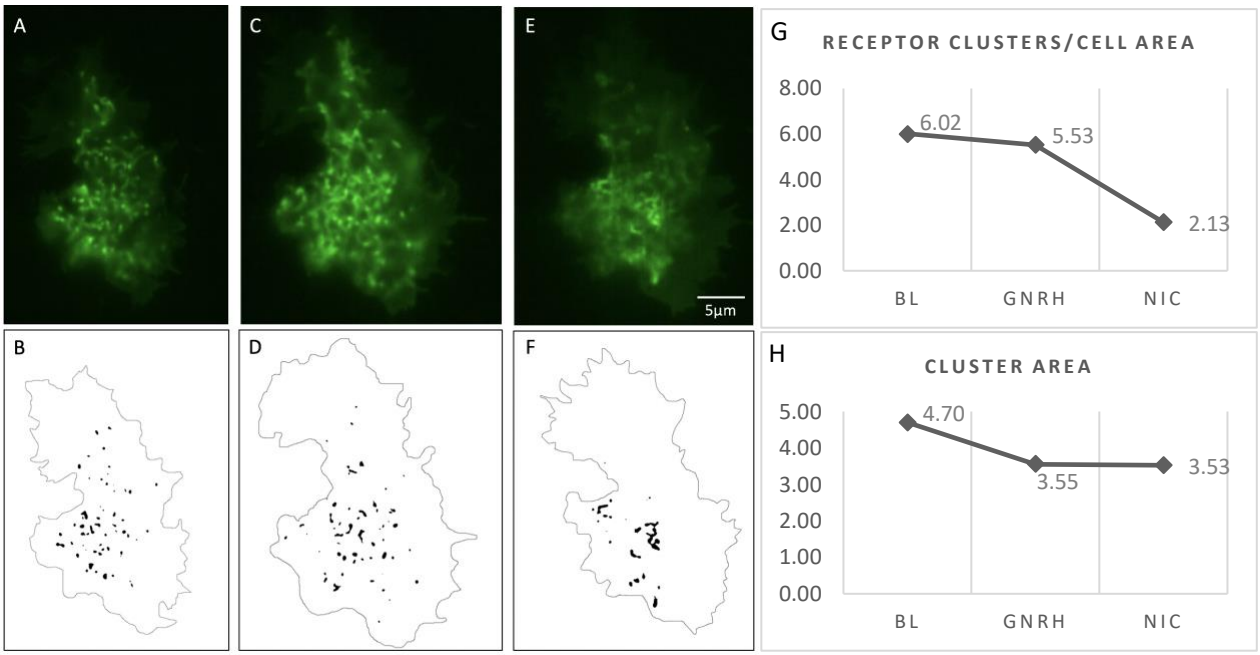

Figure 3.5 Nicardipine treatment A-B, Respective fluorescent and binary images of baseline receptor activity in calcium buffer. C-D, Same cell post-GnRH treatment. E-F, Identical cell post-FPL treatment. G, Visual representation of the cell's number of receptor clusters over total TIRF membrane area for baseline activity in calcium buffer, post-GnRH treatment, and post-FPL treatment. H, Cell's total cluster area for baseline activity in calcium buffer, post-GnRH treatment, and post-FPL treatment.

membrane field that did not show any super-resolution puncta in the baseline image. Where there were receptors before, a radial tightening can be seen, with cluster sizes becoming larger, even while the data in (H) indicates overall cluster area is decreasing. This effect became more extreme with Nic treatment (E/F), and was consistent throughout the majority of cells imaged in this condition. In fact, when normal calcium signaling was manipulated, clustering and morphology saw the most dramatic effects compared to cells treated only with GnRH, although these data are presented qualitatively through images rather than quantitatively. Representative cells demonstrating these effects are highlighted in the subsequent figures.

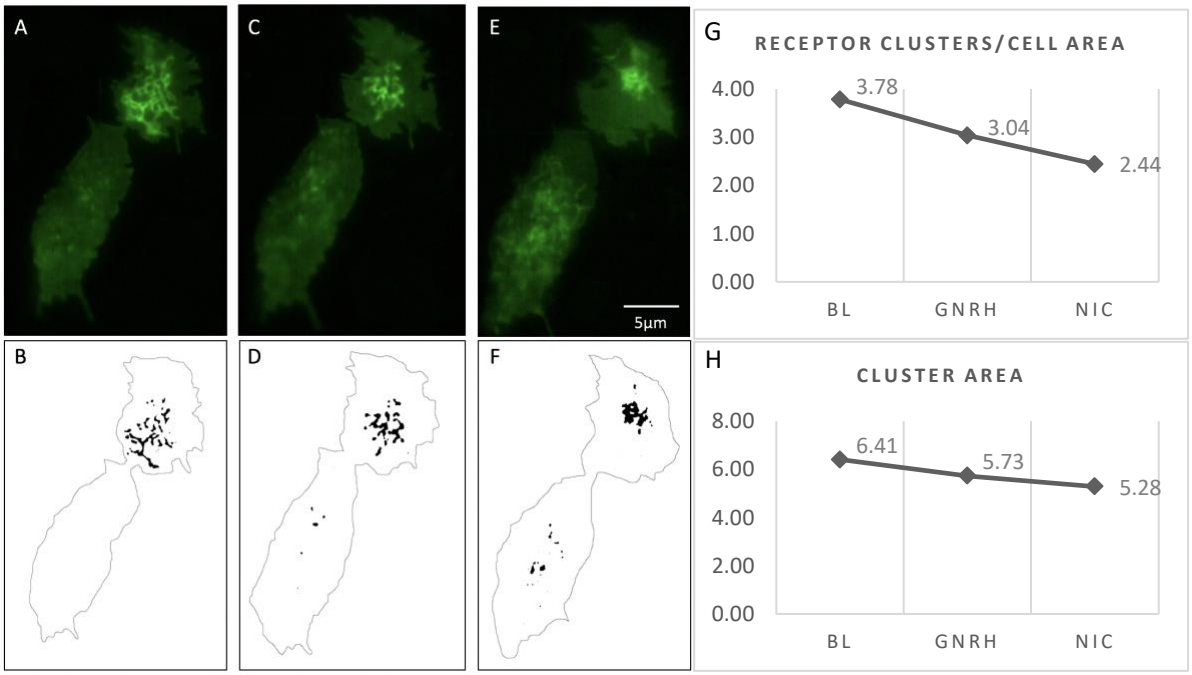

Figure 3.6 Nicardipine treatment A-B, Respective fluorescent and binary images of baseline receptor activity in calcium buffer. C-D, Same cell post-GnRH treatment. E-F, Identical cell post-Nic treatment. G, Visual representation of the cell's number of receptor clusters over total TIRF membrane area for baseline activity in calcium buffer, post-GnRH treatment, and post-Nic treatment. H, Cell's total cluster area for baseline activity in calcium buffer, post-GnRH treatment, and post-Nic treatment.

Like the previous chapter, FPL was the second drug used to modify calcium influx through L-type Ca_V channels. Number of receptor clusters over cell area were more evenly split

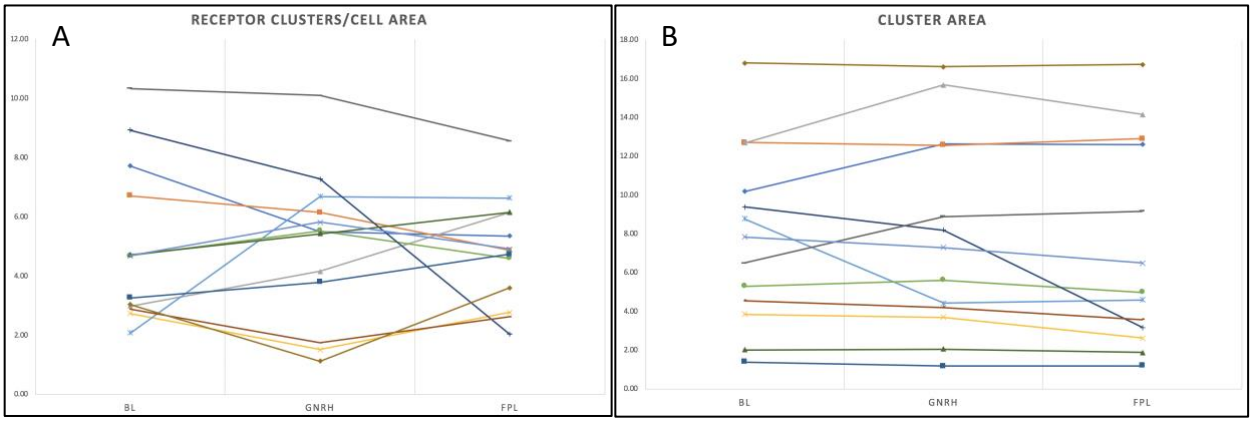

Figure 3.7 Representative data for receptor response to GnRH and FPL from baseline control images in calcium buffer. A, Normalized data showing number of receptor clusters over total membrane area in TIRF image from baseline (BL) sequences, post-GnRH treatment, and post-FPL treatment. B, Normalized binary data showing total receptor cluster area for baseline, post-GnRH, and post-FPL treatment. Colored lines represent individual cells.

in the direction of response in cells treated with FPL, while overall cluster area was less variable than other treatment groups (see figure 3.7). Visually, receptors appear to follow the same clustering behavior as the previously described GnRH and Nic-treated cells. Figure 3.8 demonstrates a perceptible increase in size of individual clusters with GnRH, although the number of clusters present has diminished thereby decreasing overall receptor area (C/D). Numerically, there is just a 0.36au difference between the baseline receptor area and the total receptor area after GnRH treatment, while the number of clusters/cell area saw a steeper decline (H). After FPL was introduced, there was a visible reduction in the disbursement of receptors (E/F), as was seen with Nic treatment.

Figure 3.9 features a second cell treated first with GnRH, and then FPL. In this image sequence, GnRH triggered new receptor areas to surface where none appeared in the baseline image (C/D). The morphology of the cell also changes slightly in the protruding “arm” allowing for more surface area to be imaged and altering the receptor to cell area ratio. After FPL treatment, the new receptor areas that surfaced with GnRH have again disappeared, but there is a

condensing in spatial distribution of receptor clusters (E/F). This is accompanied by a slight increase in total receptor area, while number of receptors/cell area still decreased (G, H).

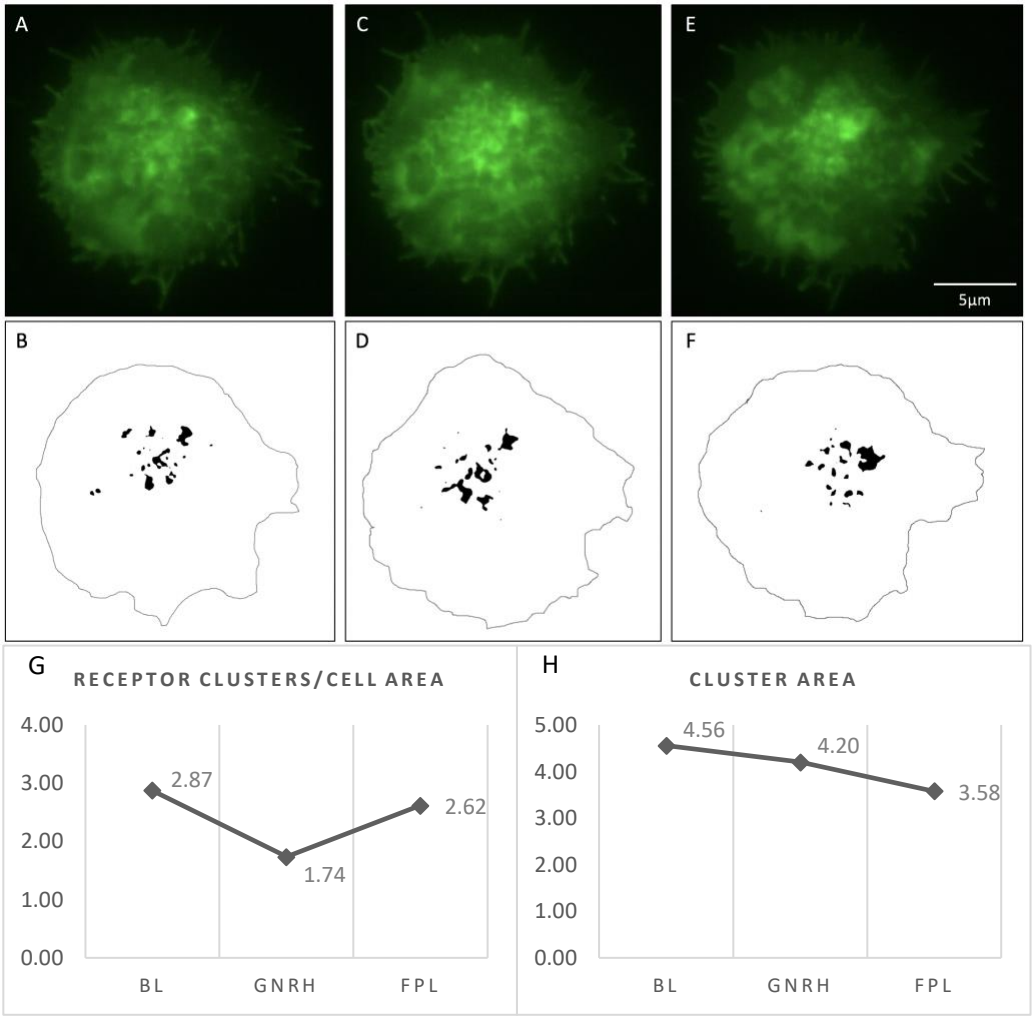

Figure 3.8 FPL treatment. A-B, Respective fluorescent and binary images of baseline (BL) receptor activity in calcium buffer. C-D, Same cell post-GnRH treatment. E-F, Identical cell post-FPL treatment. G, Visual representation of the cell's number of receptor clusters over total TIRF membrane area for baseline activity in calcium buffer, post-GnRH treatment, and post-FPL treatment. H, Cell's total cluster area for baseline activity in calcium buffer, post-GnRH treatment, and post-FPL treatment.

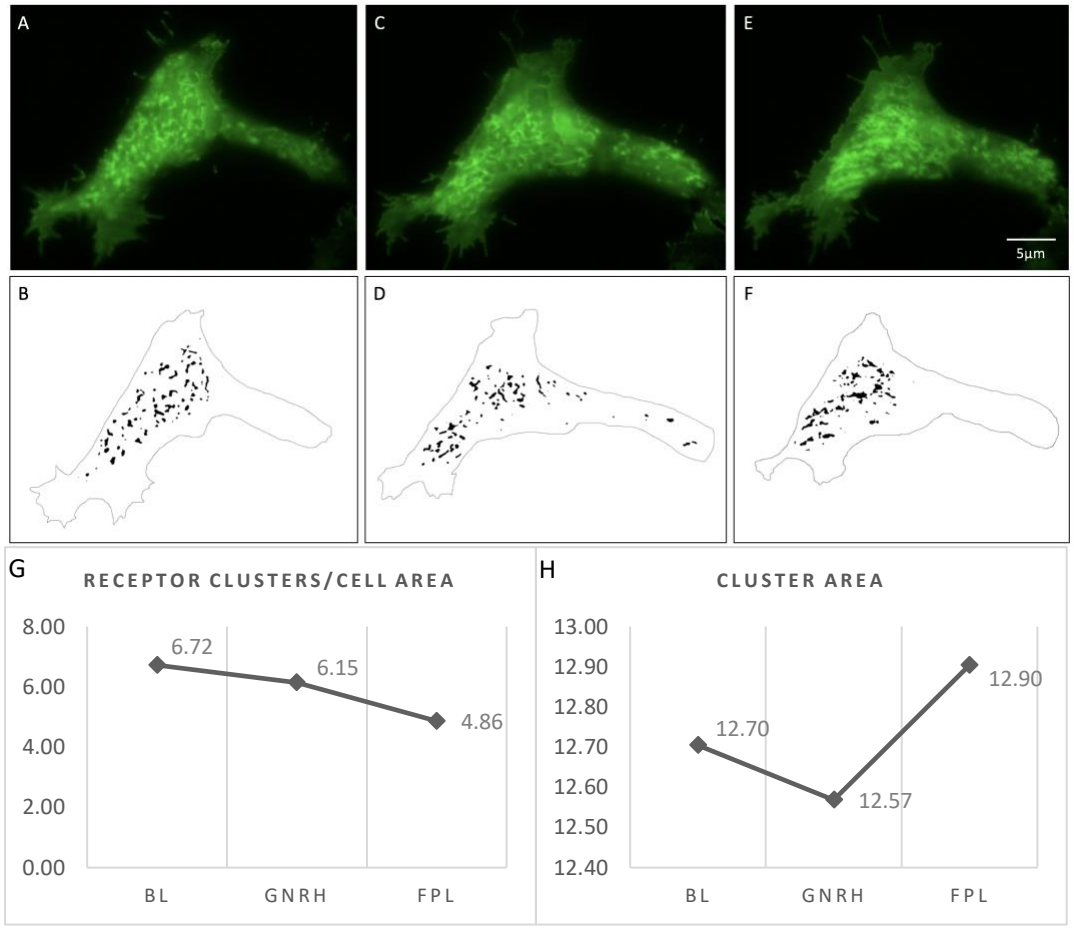

Figure 3.9 FPL treatment. A-B, Respective fluorescent and binary images of baseline (BL) receptor activity in calcium buffer. C-D, Same cell post-GnRH treatment. E-F, Identical cell post-FPL treatment. G, Visual representation of the cell's number of receptor clusters over total TIRF membrane area for baseline activity in calcium buffer, post-GnRH treatment, and post-FPL treatment. H, Cell's total cluster area for baseline activity in calcium buffer, post-GnRH treatment, and post-FPL treatment.

Finally, Thaps was used to interfere with typical intracellular calcium activity. Unlike the other treatment groups, rather than treating first with GnRH and then the drug, Thaps was used first in most dishes and then was followed by GnRH treatment. Figure 3.10 shows the receptor response in clusters/cell area and total cluster area. Results were again split among cells imaged in direction of change, but tended to reverse direction between Thaps treatment and GnRH application in both number of receptors and total cluster area, even if just slightly. Images show this effect and interestingly a different spatial pattern of receptor location on the membrane.

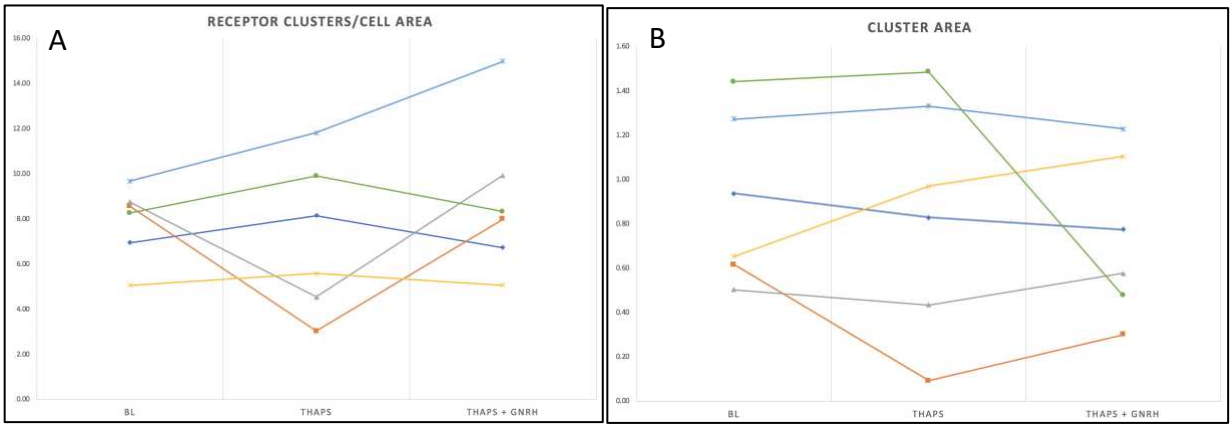

Figure 3.10 Thapsigargin Effects Representative data for receptor response to GnRH and FPL from baseline control images in calcium buffer. A, Normalized data showing number of receptor clusters over total membrane area in TIRF image from baseline (BL) sequences, post-Thapsigargin treatment, and post-GnRH treatment. B, Normalized binary data showing total receptor cluster area for baseline, post-Thapsigargin treatment, and post-GnRH treatment. Colored lines represent individual cells.

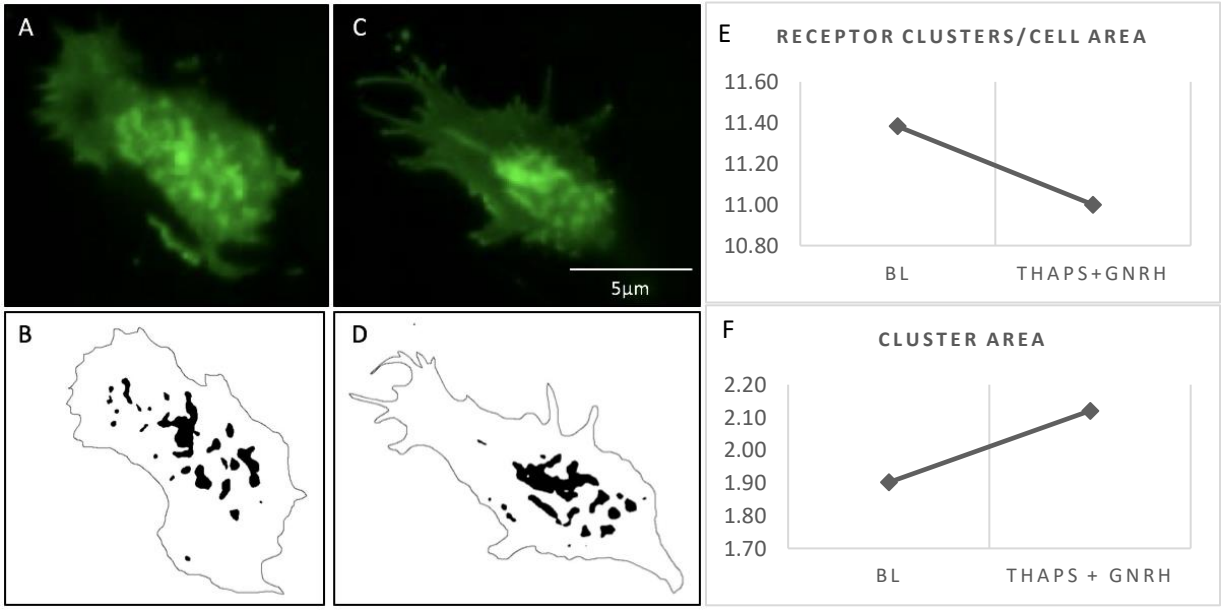

Figure 3.11 Baseline and Thapsigargin treatment with GnRH. A-B, Respective fluorescent and binary images of baseline receptor activity in calcium buffer. C-D, Same cell post-Thapsigargin treatment with GnRH added. E, Visual representation of the cell's number of receptor clusters over total cell area for baseline and post-Thaps + GnRH. F, Cell's total cluster area for baseline and post-Thaps + GnRH.

Remaining consistent with data presented thus far, figure 3.11 shows a receptor clustering pattern with GnRH even in the presence of Thaps. The cell's shape does demonstrate a more noticeable change after treatment when compared to baseline, but receptor distribution follows the same responses seen previously, with receptors congregating into larger clusters while also spatially condensing into a less-disbursed arrangement (C/D). In this particular example, there is a small decrease in receptor number/cell area (E), as well as a modest increase in total receptor area (F). This example excludes the intermediate reaction of Thaps alone, prior to hormone treatment.

Both Thaps and GnRH can be seen independently in figure 3.12, which illustrates a common morphological response seen in cells treated with Thaps. In (A), filopodia are seen projecting at the edge of the cell. In (C), after Thaps treatment, this same edge becomes "branch-like" and deformed, with far less membrane present in the TIRF field. With successive GnRH treatment (E), some of the cell's surface area is recovered, but the "branch-like" extensions are still present. Both receptor clusters/cell area and total cluster area drastically decrease after Thaps treatment, however GnRH manages to reverse this to a large extent (G, H). These "branchy" extensions and substantial decreases in membrane area in response to Thaps were seen in most cells treated or pre-incubated with the drug.

Finally, several dishes were pre-incubated with Thaps for 15 minutes before imaging. The majority of the cells in this condition saw decreases in number of receptors/cell area and total cluster area (figure 3.13). With this time of pre-incubation, cells have an opportunity to adapt to the new environment and react accordingly. This made for some varied baseline morphological observations. These cells appeared less stable on the glass bottom of their dishes, and there were many cases of the characteristic ruffling of the leading edge typically seen in

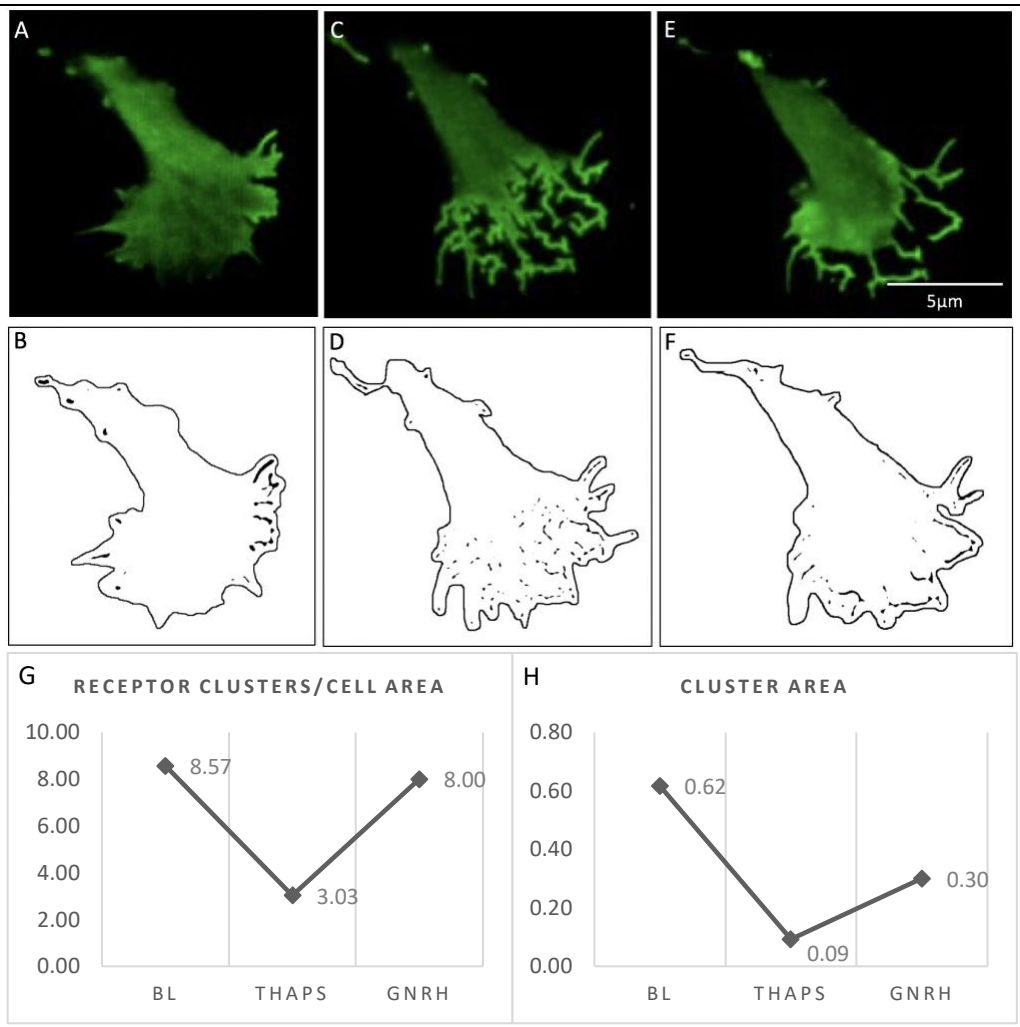

Figure 3.12 Thapsigargin treatment. A-B, Respective fluorescent and binary images of baseline receptor activity in calcium buffer. C-D, Same cell post-Thapsigargin treatment. E-F, Identical cell 10 minutes post-GnRH treatment. G, Visual representation of the cell's number of receptor clusters over total TIRF membrane area for baseline activity in calcium buffer, post-Thapsigargin treatment, and 10 minutes post-GnRH treatment. H, Cell's total cluster area for baseline activity in calcium buffer, post-Thapsigargin treatment, and 10 minutes post-GnRH treatment.

gonadotropes. These observations were drastically impacted by the addition of GnRH, where most cells exhibited the afore-mentioned "branching" behavior. This can be clearly seen in figure 3.14, where prior to GnRH treatment, the lamellipodia is perfectly extended and ruffled (A/B), whereas GnRH causes extreme withdrawal of membrane from the growth surface (C/D). In this case, both number of receptors/cell area and total cluster area decreased (E, F), although review

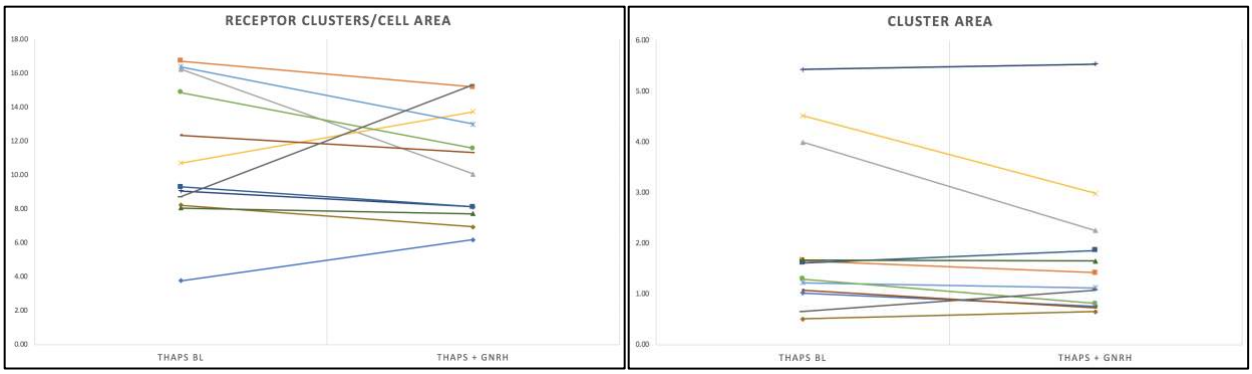

Figure 3.13 Representative data for receptor response to 15-minute Thapsigargin pre-incubation. A, Normalized data showing number of receptor clusters over total membrane area in TIRF image from baseline sequences of cells pre-incubated in Thapsigargin, and post-GnRH treatment. B, Normalized binary data showing total receptor cluster area for cells pre-incubated in Thapsigargin, and post-GnRH treatment. Colored lines represent individual cells.

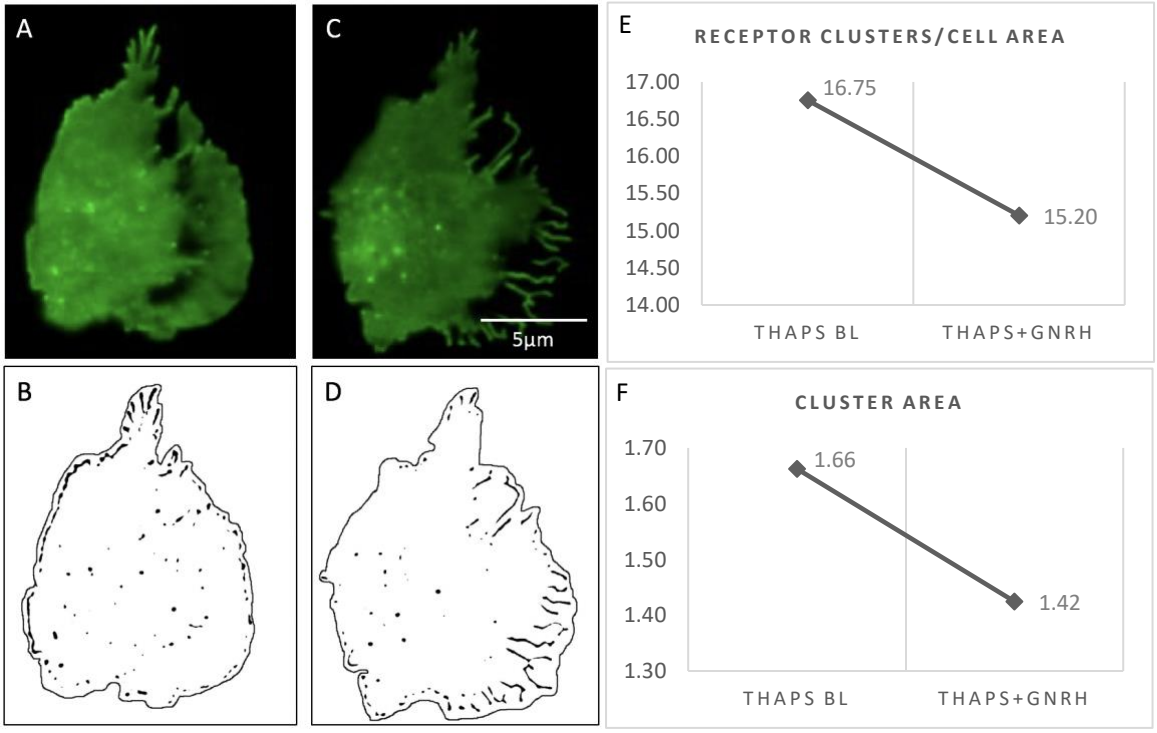

Figure 3.14 Thapsigargin pre-incubation. A-B, Respective fluorescent and binary images of cell pre-incubated with Thapsigargin for 15 minutes. C-D, Same cell 10 minutes after GnRH treatment. E, Visual representation of the cell's number of receptor clusters over total TIRF membrane area before and after GnRH treatment. F, Visual representation of the cell's total cluster area before and after GnRH treatment.

of the image itself suggests that the receptors on the body of the cell are aggregating toward a central location after GnRH treatment. While some cells still showed clear fluorescent puncta on the membrane surface, fluorescence in others was more diffuse and focused in those "branching" edges. This was the most common and notable reaction to Thaps treatment.

3.4 Discussion

After completing these experiments, there are some assumptions that can be made but further research is needed to explore different methods of analysis. First, it would appear that receptors do indeed participate in clustering activity, aggregating into larger groups, especially when normal calcium flux is altered. It is also clear that the mobile receptors do undergo spatial redistribution after activation by ligand binding, possibly increasing membrane transport and surface expression of the receptor. However, this variation in receptor behavior is accompanied by movement of the cell, changing the morphology of the membrane in the TIRF field. This makes precise analysis and quantification more challenging. The construct used is reliable and fluorescent puncta is consistently seen with adequate imaging techniques. Since one of the issues in analysis is inconsistency in quantitatively capturing the changing distribution and clustering of receptors, it would be beneficial to label and track individual receptors before and after exposure to GnRH. Single particle tracking can provide data on expressed receptor motility, organization and interaction with other receptors, and organization and interaction with other membrane-bound structures such as Ca_V channels.

In an attempt to capture receptor clustering activity upon GnRH activation, K means clustering analysis was used with binary images to assess changes in cluster distribution. This method uses vector quantization to separate and classify different points in a visual data map by the nearest mean. Each separate cluster represents a different mean, and the center point of the

cluster is labeled. Points surrounding the cluster's center are arbitrarily assigned to data points (in this case, receptor groups) and distance from the central point can be measured. Parameters are set by the researcher in terms of how many clusters to include and how many points surrounding the cluster's midpoint to analyze for distance. Beyond these parameters, the points are chosen by the model at random in order to provide a true representation of the data. In some images, the analysis worked quite well, capturing receptor cluster aggregation and radial condensing, but in others, especially those in which new receptors surfaced in cells post-GnRH treatment, the method was not appropriate. Output instead appeared as if receptors were becoming more disbursed, which was not the case. After using this method to analyze a large number of images, it was decided to be inconclusive and not included in this paper.

Morphological changes seen following drug treatment are expected with typical cell response to its environment and interaction with surrounding cells. The extreme changes in cell shape, especially with Thaps treatment, are likely due to the altered processes impacted by inhibited or extremely reduced calcium flux. Inhibition of the SERCA pump. and thus intracellular calcium release, would have consequences in membrane voltage and localized signaling dependent on minor fluctuations in concentration. As a second messenger, several mechanisms would be affected, resulting in repercussions in the cell's holistic function. As previously discussed, calcium and actin work cooperatively to regulate aspects of each other. It follows then that with altered calcium activity, the structural architecture of the cell would be compromised, as well as other functions aided by actin, such as membrane adhesion. The change seen in total membrane area before and after Thaps treatment, and then subsequent GnRH application could be explained by this.

Actin polymerization and typical cell mobility could also be impaired with the loss of proper intracellular signaling. Preliminary experiments (not pictured) looking at actin filament structure after treatment of FPL and Nic reveal fragmented pieces that are disorganized at the membrane surface. These images are starkly contrasted by those of cells treated with GnRH, where actin filaments are elongated and intentionally organized, likely to provide support for membrane proteins, receptors and organization of microdomains. These experiments should be continued, simultaneously labeling actin and the GnRH-R in order to investigate spatial interaction and organization before and after treatment. Super-resolution images could provide a foundation for further understanding receptor behavior within the context of cell movement and membrane dynamics.

Since we know that calcium and GnRH-R activity are linked, it would be interesting to investigate the spatial interaction between the receptor and L-type Ca_v channels. Immuno-staining these calcium channels and visualizing the spatial distribution and potential interaction with the GnRH-R could again provide a foundation for further understanding of membrane organization upon GnRH activation. It has been hypothesized that perhaps L-type Ca_v channels couple or aggregate into clusters with the GnRH-R upon activation. The two are functionally linked in signal generation and response, so a spatial interplay is indeed possible.

Chapter Four: Conclusion

In chapter two of this thesis, GCaMP experiments provided evidence of altered calcium activity with the treatment of GnRH, the majority of which was heightened. There also presented evidence of cell-cell communication beyond junctions, via synchronized calcium oscillations and peaking. We can conclude that descriptively, we do see more calcium flux overall with GnRH and that there is some paracellular communication taking place, especially when typical calcium signaling is impaired. This project lends itself to great potential in further understanding calcium signaling and cell-cell communication in pituitary gonadotropes. Upon collection of sufficient data in cultured cells, eventual experiments should be conducted in primary cells and slices to investigate whether observations are conserved. Eventually, a transgenic model would lead to the best results for both these experiments, and those in the following chapter.

Chapter three observations are a start to a much larger collection of experiments that will bring clarity and understanding to the structural and functional arrangement of expressed GnRH receptors at the membrane. We can qualitatively conclude that receptors do display clustering/aggregate behavior in the presence of GnRH, especially when normal calcium signaling is impaired. More in-depth research and appropriate analytical methods are needed to further explore these observations, but these data do support previous assumptions surrounding receptor response to hormone activation.

Overall, calcium is a critically important second messenger in gonadotropes, impacting many facets that are observable through experimentation. Although cellular processes and their underlying mechanisms have proven to be more complex than initially thought, the data herein may provide a stepping stone for others to expand on, creating a more in-depth understanding of gonadotropic function in the larger system.

References

Aguilar-Rojas, A., Pérez-Solis, M. A., & Maya-Núñez, G. The gonadotropin-releasing hormone system: Perspectives from reproduction to cancer (Review). (2016). *International Journal of Oncology 48*(3), 861-868. doi:10.3892/ijo.2016.3346

Beta, C. & Kruse, K. (2017). Intracellular oscillations and waves. *Annual Review of Condensed Matter Physics 8*, 239-264. doi:10.1146/annurev-conmatphys-031016-025210

Bliss, S. P, Navratil, A. M., Xie, J., Roberson, M. S. GnRH signaling, the gonadotrope and endocrine control of fertility. (2010). *Frontiers in neuroendocrinology 31*(3), 322-340. doi:10.1016/j.yfrne.2010.04.002

Campos, P., Golan, M., Hoa, O., Fiordelisio, T., & Mollard, P. (2018). Pituitary cell and molecular. In: Skinner, M. K. (Ed.) *Encyclopedia of Reproduction (2nd ed.)*.

Catterall, W. A. Voltage-gated calcium channels. (2011). *Cold Spring Harbor perspectives in biology,* 3:a003947. doi:10.1101/cshperspect.a003947

Cheng, C. K., & Leung, P. C. K. (2005). Molecular biology of gonadotropin-releasing hormone (GnRH)-I, GnRH-II, and their receptors in humans. *Endocrine Reviews 26*(2), 283–306. doi:10.1210/er.2003-0039

Chowdhury, I., & Sridaran, R. GnRH-GnRH-Receptor system in the mammalian female reproductive tract. (2009) In: Chedrese PJ, *Reproductive Endocrinology: A Molecular Approach*. 131-143. Springer. doi:10.1007/978-0-387-88186-7_13

Dalghi, M. G., Ferreira-Gomes, M., & Rossi, J. P. (2018). Regulation of the plasma membrane calcium ATPases by the actin cytoskeleton. *Biochemical and Biophysical Research Communications 506*(2), 347-354. doi:10.1016/j.bbrc.2017.11.151

Dang, A. K., Chaplin, N. L., Murtazina, D. A., Boehm, U., Clay, C. M., & Amberg, G. C.

(2018). Subplasmalemmal hydrogen peroxide triggers calcium influx in gonadotropes. *Journal of Biological Chemistry 293*(41), 16028–16042.

Dravid, S. M., & Murray, T. F. (2004). Spontaneous synchronized calcium oscillations in neocortical neurons in the presence of physiological [Mg2+]: involvement of AMPA/kainate and metabotropic glutamate receptors. *Brain Research 1006*(1), 8-17. doi:10.1016/j.brainres.2004.01.059

Fletcher, P. A., Sherman, A., & Stojilkovic, S. S. (2018). Common and diverse elements of ion channels and receptors underlying electrical activity in endocrine pituitary cells. *Molecular and Cellular Endocrinology 463*, 23-36. doi:10.1016/j.mce.2017.06.022

Grosse, R., Schmid, A., Schöneberg, T., Herrlich, A., Muhn, P., Schultz, G., & Gudermann, T. (2000). Gonadotropin-releasing hormone receptor initiates multiple signaling pathways by exclusively coupling to Gq/11 proteins. *The Journal of biological chemistry 275*(13), 9193-9200. doi:10.1074/jbc.275.13.9193

Gu, H., Pan, B., & Xu, J. (2014). Experimental observation of spike, burst and chaos synchronization of calcium concentration oscillations. *Europhysics Letters 106*(5). doi: 10.1209/0295-5075/106/50003

Haisenleder, D. J., Yasin, M., & Marshall, J. C. (1997). Gonadotropin subunit and gonadotropin-releasing hormone receptor gene expression are regulated by alterations in the frequency of calcium pulsatile signals*. *Endocrinology 138*(12), 5227-5230. doi: 10.1210/endo.138.12.5611

Hall, J. E., Taylor, A. E., Hayes, F. J., & Crowley, W. F. Insights into hypothalamic-pituitary dysfunction in polycystic ovary syndrome. (1998). *Journal of endocrinological investigation 21*. 602-611.

Hartzell, C. A., Jankowska, K. I., Burkhardt, J. K., & Lewis, R. S. (2016). Calcium influx through CRAC channels controls actin organization and dynamics at the immune synapse. *eLife*. 5:e14850. doi:10.7554/eLife.14850

Höfer, T. (1999). Model of intercellular calcium oscillations in hepatocytes: synchronization of heterogeneous cells. *Biophysical Journal 77*(3), 1244-1256. doi:10.1016/S0006-3495(99)76976-6

Horvat, R.D., Roess, D.A., Nelson, S.E., Barisas, B.G., & Clay, C.M. (2001). Binding of agonist but not antagonist leads to fluorescence resonance energy transfer between intrinsically fluorescent gonadotropin-releasing hormone receptors. *Molecular Endocrinology 15*(5), 695–703.

Lombó, M., Fernández-Díez, C., González-Rojo, S., Navarro, C., Robles, & Paz Herráez, M. (2015). Transgenerational inheritance of heart disorders caused by paternal bisphenol A exposure. *Environmental Pollution 206*. 667-678. doi: 10.1016/j.envpol.2015.08.016

Melamed, P., Savulescu, D., Lim, S., Wijeweera, A., Luo, Z., Luo, M., & Pnueli, L. (2012). Gonadotrophin-releasing hormone signaling downstream of calmodulin. *Journal of Neuroendocrinology 24*(12), 1463–1475. doi:10.1111/j.1365-2826.2012.02359.x

Merelli, F., Stojilkovic, S. S., Iida, T., Krsmanovic, L. Z., Zheng, L., Mellon, P. L., and Catt, K. J. (1992). Gonadotropin-releasing hormone-induced calcium signaling in clonal pituitary gonadotrophs. *Endocrinology 131*(2), 925–932.

Mulvaney, J. M., & Roberson, M. S. (2000). Divergent Signaling Pathways Requiring Discrete calcium Signals Mediate Concurrent Activation of Two Mitogen-activated Protein Kinases by Gonadotropin-releasing Hormone. *The Journal of Biological Chemistry 275*, 14182-14189. doi:10.1074/jbc.275.19.14182

Mulvaney, J. M., Zhang, T., Fewtrell, C., & Roberson, M. S. (1999). Calcium influx through L-type channels is required for selective activation of extracellular signal-regulated kinase by gonadotropin-releasing hormone. *The Journal of Biological Chemistry 274*(42), 29796–29804.

Nakai, J., Ohkura, M., & Imoto, K. (2001). A high signal-to-noise Ca(2+) probe composed of a single green fluorescent protein. *Nature Biotechnology 19*(2), 137–141. doi:10.1038/84397

Naor, Z. (2009). Signaling by G-protein-coupled receptor (GPCR): studies on the GnRH receptor. *Frontiers in Neuroendocrinology 30*(1):10–29. doi:10.1016/j.yfrne.2008.07.001

Navratil, A. M., Bliss, S. P., Berghorn, K. A., Haughian, J. M., Farmerie, T. A., Graham, J. K., Clay, C. M., & Roberson, M. S. (2003). Constitutive localization of the gonadotropin-releasing hormone (GnRH) receptor to low density membrane microdomains is necessary for GnRH signaling to ERK. *The Journal of Biological Chemistry 278*, 31593-31602. doi:10.1074/jbc.M304273200

Navratil, A. M., Bliss, S. P., & Roberson, M. S. (2010). Membrane rafts and GnRH receptor signaling. *Brain research 1364*. 53-61. doi: 10.1016/j.brainres.2010.09.008

Navratil, A. M., Dozier, M. G., Whitesell, J. D., Clay, C. M., & Roberson, M. S. (2014). Role of cortactin in dynamic actin remodeling events in gonadotrope cells. *Endocrinology 155*. 548-557. doi:10.1210/en.2012-1924

Navratil, A. M., Knoll, J. G., Whitesell, J. D., Tobet, S. A., & Clay, C. M. (2007). Neuroendocrine plasticity in the anterior pituitary: gonadotropin-releasing hormone-mediated movement in vitro and in vivo. *Endocrinology 148*. 1736-1744. doi:10.1210/en.2006-1153

Paulose, T., Speroni, L., Sonnenschein, C., & Soto, A. M. (2015). Estrogens in the wrong place at the wrong time: Fetal BPA exposure and mammary cancer. *Reproductive Toxicology 54*. 58-65. doi: 10.1016/j.reprotox.2014.09.012

Plant, T. M. (2015). 60 years of neuroendocrinology: the hypothalamo-pituitary-gonadal axis. *Journal of Endocrinology 226*, T41–T54. doi:10.1530/joe-15-0113

Powell J., Falcke M., Skupin A., Bellamy T.C., Kypraios T., & Thul R. (2020). A statistical view on calcium oscillations. In: Islam, M. S. (Ed.) Calcium Signaling. *Advances in Experimental Medicine and Biology v. 1131*. 799-826. Springer, Cham. doi:10.1007/978-3-030-12457-1_32

Reame, N. E., Sauder, S. E., Case, G. D., Kelch, R. P., & Marshall, J. C. (1985). Pulsatile gonadotropin secretion in women with hypothalamic amenorrhea: evidence that reduced frequency of gonadotropin-releasing hormone secretion is the mechanism of persistent anovulation. *The Journal of clinical endocrinology and metabolism 61*. 851-858

Richter, T. A., Keen, K. L., & Terasawa, E. (2002). Synchronization of Ca^{2+} oscillations among primate LHRH neurons and nonneuronal cells in vitro. *Journal of Neurophysiology 88*, 1559–1567. doi:10.1152/jn.00805.2001

Rispoli, L. A., & Nett, T. M. (2005). Pituitary gonadotropin-releasing hormone (GnRH) receptor: Structure, distribution and regulation of expression. *Animal Reproduction Science 88*(1–2), 57-74. doi: 10.1016/j.anireprosci.2005.05.004

Ruffinatti, F.A. Gilardino, A. Secchi, V. Cottone, E. Lovisolo, D. & Bovolin, P. (2019) Bisphenol A activates calcium influx in immortalized GnRH neurons. *International Journal of Molecular Sciences 20*(9). 2160. doi:10.3390/ijms20092160

Simons, K., & Vaz, W. (2004). Model systems, lipid rafts, and cell membranes. *Annual Review*

of Biophysics and Biomolecular Structure 33, 269-295. doi: 10.1146/annurev.biophys.32.110601.141803

Sezgin, E., Levental, I., Mayor, S., & Eggeling, C. (2017). The mystery of membrane organization: composition, regulation and roles of lipid rafts. *Nature Reviews Molecular Cell Biology 18*, 361–374. doi: 10.1038/nrm.2017.16

Stojilkovic, S. S., Bjelobaba, I., & Zemkova, H. (2017). Ion channels of pituitary gonadotrophs and their roles in signaling and secretion. *Frontiers in Endocrinology 8*(126). doi:10.3389/fendo.2017.00126

Stojilkovic, S. S., Tabak, J., & Bertram, R. (2010). Ion channels and signaling in the pituitary gland. *Endocrine Review 31*(6), 845–915. doi:10.1210/er.2010-0005

Tang, E., & Zuo, H. (2017). Simulations to evaluate the impact of Ca2+ release from endoplasmic reticulum on intracellular Ca2+ oscillations. *Advances in Intelligent Systems Research 153*. 211-214. doi:10.2991/amms-17.2017.47

Themmen A. P. N., & Huhtaniemi I. T. (2000). Mutations of gonadotropins and gonadotropin receptors: elucidating the physiology and pathophysiology of pituitary-gonadal function. *Endocrine Reviews 21*. 551-583

Thurley, K., Skupin, A., Thul, R., & Falcke, M. (2012). Fundamental properties of Ca2+ signals. *Biochimica et Biophysica Acta (BBA)-General Subjects 1820*(8), 1185–1194. doi:10.1016/j.bbagen.2011.10.007

Tomao, F., Russo, G. L., Spinelli, G. P., Stati, V., Prete, A. A., Prinzi, N., Sinjari, M., Vici, P., Papa, A., Chiotti, M. S., Panici, P. B., Tomao, S. (2014). Fertility Drugs, Reproductive Strategies and Ovarian Cancer Risk. *Journal of Ovarian Research 7*(51). doi:10.1186/1757-2215-7-51.

Tsai, F. C., Seki, A., Yang, H. W., Hayer, A., Carrasco, S., Malmersjo, S., & Meyer, T. (2014). A polarized Ca^{2+}, diacylglycerol and STIM1 signaling system regulates directed cell migration. *Nature Cell Biology 16*(2), 133-144. doi:10.1038/ncb2906.

Tsutsumi, R. & Webster, N. J. G. (2009). GnRH Pulsatility, the Pituitary Response and Reproductive Dysfunction. *Endocrine Journal 56*(6), 729-737.

Wang, Q., Shui, B., Kotlikoff, M. I., & Sondermann, H. (2008). Structural basis for calcium sensing by GCaMP2. *Structure 16*(12), 1817–1827. doi:10.1016/j.str.2008.10.008

Wang, X., & Gruenstein, E. I. (1997). Mechanism of synchronized Ca2+ oscillations in cortical neurons. *Brain Research 767*(2), 239-249. doi:10.1016/S0006-8993(97)00585-4

Willars, G. B., Heding, A. Vrecl, M., Sellar, R., Blomenrohr, M., Nahorski, S. R., & Eidne, K.A. (1999). Lack of a C-terminal tail in the mammalian gonadotropin-releasing hormone receptor confers resistance to agonist-dependent phosphorylation and rapid desensitization. *Journal of Biological Chemistry 274*, 30146-30153.

Zhang, B., Fendler, B., Peercy, B., Goel, P., Bertram, R., Sherman, A., & Satin, L. (2008). Long lasting synchronization of calcium oscillations by cholinergic stimulation in isolated pancreatic islets. *Biophysical Journal 95*(10), 4676-4688. doi:10.1529/biophysj.107.125088

Appendix

Representative videos of the GCaMP experiments from chapter 2 can be found at the following links:

Cell group example 1 post-GnRH treatment: https://youtu.be/qyw443LWbWw

Cell group example 2 post-GnRH treatment: https://youtu.be/mUGsJytkmXo

Cell group 1 baseline: https://youtu.be/hFBlPmB4_3Y

Cell group 1 post-GnRH: https://youtu.be/yAAzcKaN6eM

Cell group pre-incubated with Nicardipine baseline: https://youtu.be/MMm891Dumd8

Cell group pre-incubated with Nicardipine post-GnRH: https://youtu.be/GCa8ZNhIiBQ

Cell group 2 post-GnRH: https://youtu.be/pNgoFG6N5Js

Cell group 2 post-GnRH + Nicardipine: https://youtu.be/IPTJhSjAEi8

Cell group 3 baseline: https://youtu.be/C6BKhsNPv98

Cell group 3 post-GnRH: https://youtu.be/HVwLnF6zbdE

Cell group 3 post-GnRH + Thapsigargin: https://youtu.be/ub9GqfFC8tM